ABSTRACT

Title of dissertation: INITIAL STATE PREPARATION FOR SIMULATION OF QUANTUM FIELD THEORIES ON A QUANTUM COMPUTER

Ali Hamed Moosavian
Doctor of Philosophy, 2019

Dissertation directed by: Professor Stephen Jordan
Department of Physics

In this thesis, we begin by reviewing some of the most important Hamiltonian simulation algorithms that are applied in simulation of quantum field theories. Then we focus on state preparation which has been the slowest subroutine in previously known algorithms. We present two distinct methods that improve upon prior results. The first method utilizes classical computational tools such as Density Matrix Renormalization Group to produce an efficient quantum algorithm for simulating fermionic quantum field theories in 1+1 dimensions. The second method presented is a heuristic algorithm that can prepare the vacuum of fermionic systems in more general cases and more efficiently than previous methods. With our last method, state preparation is no longer the bottleneck, as its runtime has the same asymptotic scaling with the desired precision as the remainder of the simulation algorithm. We then numerically demonstrate the effectiveness of this last method for the 1+1 dimensional Gross-Neveu model.

INITIAL STATE PREPARATION FOR SIMULATION OF QUANTUM FIELD THEORIES ON A QUANTUM COMPUTER

by

Ali Hamed Moosavian

Dissertation submitted to the Faculty of the Graduate School of the
University of Maryland, College Park in partial fulfillment
of the requirements for the degree of
Doctor of Philosophy
2019

Advisory Committee:
Professor Andrew Childs, Chair/Co-Advisor
Professor Stephen Jordan, Advisor
Professor Zohreh Davoudi
Professor Brian Swingle
Professor Mohammad Hafezi

Dedication

"...He hath distinguished you, and hath not placed upon you any narrowness in the religion the faith of your *father*, Abraham..."

Quran 22:78

I believe the notion of parenthood is greater than being limitd to just biological parents. This work is dedicated to all of my parents.

Acknowledgments

"*The person among you whom thanks the others the most is the one whom thanks God the most.*"

Ali Ibn Al-Hussain

It might be possible to finish some things individually, however, my PhD and this dissertation is definitely not one of them. Here, I would like to thank the people that I owe greatly.

First and foremost I would like to thank my parents, my grandparents and my brother for their continuous and endless love and support throughout my life.

Special thanks would go to my advisor, Stephen Jordan, for invaluable advice and support. He was not only a great mentor in research, but I learned invaluable lessons from him about life. His positive and welcoming attitude has motivated me time and time again. It has been a great pleasure to work with such an extraordinary individual.

From elementary school until the end of my undergraduates, my education has been almost entirely in Iran. I am grateful for having nothing but exceptional teachers and professors throughout this time. The list is long, but specifically I would like to thank some of my notable teachers whom helped my talents flourish and encouraged me to persue them, Hassan Najafizadeh, Hashem Miri, and Ahmad Ghodsi.

I am also grateful to have participated in Perimeter Scholars International program. It was a privilege to learn from some of the brightest physicists in the

world. In particular I would like to thank Daniel Gottesman for a brilliant course and wonderful mentoring that helped me shape my career.

During my time in University of Maryland I've had the privilege to work with and learn from brilliant professors via classes and collaborations. In particular I would like to thank Alexey Grorshkov, Andrew Childs, Michelle Girvan, Brian Swingle, Zohreh Davoudi and Raman Sundrum. I would also like to thank James Garrison, Mohammad Maghrebi and Zhe-Xuan Gong for making themselves available and giving great advice and helpful company whenever I needed it.

I would also like to thank Robin Kothari, Ali Lavasani, Guang Hao Low, Yannick Meurice, John Preskill, Seth Whitsitt, Norbert Schuch, Scott Glancy, and members of the theoretical Quarks, Hadrons and Nuclei group at the Maryland Center for Fundamental Physics for helpful discussions.

I would also like to thank my friends, Jeremy Young, Abhinav Deshpande, Stephen Ragole and Andrew Glaudell whom I've shared an office with for several years. They have been a great source of academic on non-academic conversations. I would also like to thank my friends Ali Lavasani, Alireza Parhizkar, Alireza Seif, Ali Izadi Rad, Batool Banihashemi, Troy Sewell, Aaron Ostrander, Majid Ekhterachian, Yidan Wang, Meghdad Yazdanpanah, Yahya Alavirad, Mehdi Kohani, Peyman Yousefian and Hossein Dehghani for their friendship and support.

Heartfelt thanks would go to all of my friends at UMD's unofficial Quran session. They helped me remain spiritually and mentally intact during this period.

Last but definitely not least, I owe more thanks than can fit in these pages to my wife, Fatemeh. She has continuously loved and supported me despite all the

problems we had to face.

Table of Contents

List of Tables

List of Figures

List of Abbreviations

BQP	Bounded-error Quantum Polynomial time
DMRG	Density Matrix Renormalization Group
IC	Integrated Circuit
LCU	Linear Combination of Unitaries
LQCD	Lattice Quantum Chromodynamics
MPO	Matrix Product Operator
MPS	Matrix Product State
NISQ	Noisy Intermediate-Scale Quantum
PEPS	Projected Entangled Pair States
QCD	Quantum Chromodynamics
QFT	Quantum Field Theory
RWA	Rotating Wave Approximation
SM	Sparse Matrix
SVD	Singular Value Decomposition

Citations to Previously Published Work

Some of this dissertation appeared in papers already published. Here we outline those publications.

- Chapter 3: Hamed Moosavian, A., & Jordan, S. (2018). Faster quantum algorithm to simulate fermionic quantum field theory. Physical Review A, 98(1), 012332. https://doi.org/10.1103/PhysRevA.98.012332

- Chapter 4: Hamed Moosavian, A., Garrison, J. R., & Jordan, S. P. (2019). Site-by-site quantum state preparation algorithm for preparing vacua of fermionic lattice field theories. arXiv: 1911.03505

Chapter 1: Introduction

1.1 Historical motivation for quantum simulation algorithms

> "*Nature isn't classical, dammit, and if you want to make a simulation of nature, you'd better make it quantum mechanical, and by golly it's a wonderful problem, because it doesn't look so easy.*"
>
> Richard P. Feynman

In general to simulate a process or a system means to approximately imitate its behavior over time. This often involves generating a history of a set of characteristics of the system of interest. A *simulation model* is used to observe the constraints and the dynamical interplay of these characteristics [Ban+10; Pau87].

Beginning by some of the pioneering Monte-Carlo simulations done in the Manhattan project, computer simulation methods and its applications have evolved over time and grown immensely. Figure 1.1 shows the rapid increase in the frequency that the word *simulation* has appeared in written contexts over time. This rapid growth is a natural result of the wide range of applications computer simulations have found. In many cases computer simulations have become a cost saving part of research. Some of the benefits of simulation as a low-cost and low-risk replacement

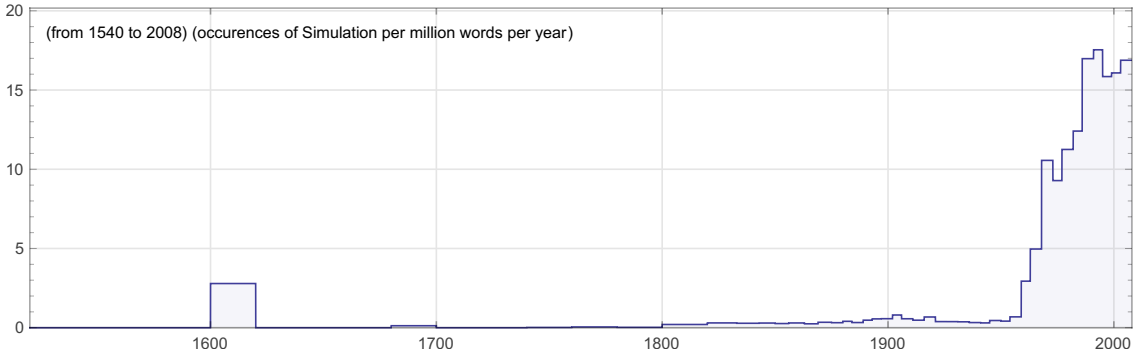

Figure 1.1: (color online) The frequency that the word *simulation* has been used over time. The plot is based on [Mic+11].

for experimentation are as follows [Ban+10]:

1. Simulations can enable the study of the internal interactions in a complex system, which could be otherwise hard or in some cases impossible.

2. Simulations can be used to verify the theoretical model. Examples of these simulations can be seen in [Abb+16; Sir+18].

3. Sometimes going through with an experiment would risk huge environmental and ecological impacts. In these cases one needs to do a simulation to study these impacts and prepare for the possible outcomes.

4. Computer simulations can be used in pedagogical contexts too. They can be used to familiarize students with different potentially dangerous subjects or train pupils for a task without the possible risks and costs associated with that task.

Just to name a few, some applications where classical simulations are widely used are: Weather forecasting [Mol+96], power system simulation [Jay16], reservoir simulation [PHD05] and traffic engineering [Pur98].

No matter how successful classical simulation algorithms seem to be, they inherently lack the power to efficiently simulate some of the most underlying systems in the nature. The problem is that the underlying systems in our universe are inherently quantum rather than classical. The classical memory required to even store a generic quantum state grows exponentially with the number of sites. This means in order to accurately store the quantum state of the cheese one has for breakfast, a classical memory with as many bits as the particles in the known universe would not suffice. Just to put this fact into perspective, the particles in the known universe are dominated vastly by photons. If one hypothetically had access to all the photons in the known universe and could use them to store classical data bits, they would only be able to represent the state of 296 spin-$\frac{1}{2}$ particles [HMS18]. Many molecules that are used in pharmacology have vastly more elementary particles than that. There are some classical techniques to store and process some quantum states more efficiently; which we will discuss briefly in Chapters 3 and 4. However, most quantum states do not fall into those categories.

That is why in the 1980s, scientists like Richard Feynman and David Deutsch started to think about alternative models of computation that do not suffer from the same limitations, namely quantum computers [Fey82; Fey85; Deu85a; Deu89]. One of the main motivations for pursuing quantum computation to simulate quantum systems is the fact that any discrete quantum state can be efficiently represented on it. The biggest concern at the time was whether it is possible to retain coherent qubits in the presence of noise (For example see [Unr95]). These concerns were later addressed in the years 1995 and 1996 by seminal works of Peter Shor and Andrew

Steane [Sho95; Sho96; DS96; Ste96b; Ste96a]. They showed the possibility of retaining coherent states by using error correction methods. Within a few years fully fault-tolerant protocols were conceptualized and threshold theorems were proven [Pre98; KLZ96; KLZ98; Got98].

In 1996 Seth Lloyd showed that the evolution of local Hamiltonians can be simulated on a universal quantum computer with at most polynomial overhead [Llo96]. It is safe to say that this important result sparked a lot of ideas for using quantum devices to simulate quantum systems. We will discuss some of these results in Secs. 1.2 and 1.3.

We would like to finish this section of the introduction by mentioning that in the past decade there has been ongoing research for developing quantum simulation algorithms for classical systems too. Some of the noteworthy ones, with super-polynomial speedups, are simulation problems that reduce to solving a linear equation. For example see [CJO19; CPP13].

1.2 Quantum simulators

Quantum simulation devices can be grouped into two main categories, analog simulators and digital simulators. We will discuss each of these in the following Secs. 1.2.1 and 1.2.2.

1.2.1 Analog Quantum Simulation

A natural approach to the simulation problem is to start with a highly tunable physical system and finely adjust its Hamiltonian until it approximates the Hamiltonian of the system we are interested in simulating. For instance, ultracold atoms have been particularly successful in this regards [Mac12; Ban+12; Ric+18; Kas+17; ZCR15; Haf+07; Ber+17]. The reasons why cold atoms are so successful are as follows [BDN12]:

1. Atoms are fairly isolated from the environment.

2. Their interactions can be finely tuned using electromagnetic fields and Feshbach resonances.

3. It is possible to make theoretical predictions starting from first principles.

4. Some of the coldest temperatures ever recorded are accessible in these systems by using laser cooling.

Another successful approach for an analog quantum simulator would be to use trapped ions [Zha+17; BR12]. Again, being able to finely engineer the interactions and long decoherence times are the main selling points for these analog simulators.

Despite their proven success, analog quantum simulators have their fair share of limitations as well. Just to name a few, often the simulation device has to be engineered and tailored towards the very specific system it is intended to simulate. Besides that the in most cases they are limited by their geometrical structure and can

only allow very few types of interactions. Another issue is that in the analog systems there is no notion of error correction and fault tolerance. These are the reasons why we believe after large scale universal quantum computers become available, they would eventually replace the analog simulators.

1.2.2 Digital Quantum Simulation

As David Deutsch showed in 1985, an alternative approach to the analog strategy is to build a quantum device that only needs to implement a universal yet small number of quantum gates [Deu85a]. The notion of universality here means that any unitary operator can be ϵ-approximated using only the finite gates in the set [NC00]. An example of a universal set of quantum gates represented in the standard basis would be:

$$H = \frac{1}{\sqrt{2}} \begin{pmatrix} 1 & 1 \\ 1 & -1 \end{pmatrix} , \tag{1.1}$$

$$R_Z\left(\frac{\pi}{4}\right) = \begin{pmatrix} 1 & 0 \\ 0 & e^{i\pi/4} \end{pmatrix} , \tag{1.2}$$

$$CNOT = \begin{pmatrix} 1 & 0 & 0 & 0 \\ 0 & 1 & 0 & 0 \\ 0 & 0 & 0 & 1 \\ 0 & 0 & 1 & 0 \end{pmatrix} . \tag{1.3}$$

Although the above set of gates is universal, all of them cannot be implemented

fault-tolerantly without some extra resources. However, there are techniques such as magic state distillation which can be utilized to yield fault-tolerance and universality simultaneously [Vei+14; Rei06; CAB12; Rei05; CTV17; CB09; MEK12; Haa+17].

The universal approach to quantum computation has plenty of benefits over the analog equivalents. First of all, the experimentalists can focus on implementing just a few gates instead of building a new Hamiltonian from scratch each time a new problem arises. The other important feature of digital quantum computation is that once the accuracies of the gates reach a threshold value, the overall outcome error can be arbitrarily suppressed [KLZ96]. In Sec. 1.3 we will explain some of the algorithms for Hamiltonian simulation using this latter notion.

1.3 Hamiltonian Simulation algorithms

The statement of the Hamiltonian simulation problem is that given a Hamiltonian H, find a quantum circuit that approximates the unitary operator $U = e^{-iHt}$ with a maximum error, ϵ. Depending on the context of a specific algorithm, this error can be defined using various distance measures such as trace distance. As it is evident from Table 1.1 Hamiltonian simulation has been an active area of research in the quantum computation community. I will explain some of the more pedagogically important results in a chronological order in the following sections.

Year	Paper	Performance
2019	[LKW19]	$\tilde{O}\left(t\sum_{j=1}^{N}\left\|h_j\right\|\right)$ *
2019	[Ber+19]	$\tilde{O}\left(\left(d\left\|H\right\|_{\max,1}\right)n\right)$ $\tilde{O}\left(\left\|\alpha\right\|_{\infty,1}L^2 g_c\right)$
2019	[CS19]	$O\left(\frac{(nt)^{1+\frac{1}{p}}}{\epsilon^{\frac{1}{p}}}\right)$
2018	[Haa+18]	$O\left(nt\,\mathrm{polylog}\left(\frac{nt}{\epsilon}\right)\right)$
2016	[LC16a]	$\tilde{O}\left(t\sqrt{d\left\|H\right\|_{\max}\left\|H\right\|_1}\right)$ *
2016	[LC16b]	$O\left(td\left\|H\right\|_{\max}+\frac{\log\left(\frac{1}{\epsilon}\right)}{\log\left(\log\left(\frac{1}{\epsilon}\right)\right)}\right)$ *
2016	[BN16]	$O\left(t\left\|H\right\|_{\max}d\frac{\log\log\left(t\|H\|_{\max}d\right)}{\log\log\log\left(t\|H\|_{\max}d\right)}+\log 1/\left(\epsilon\right)\right)$ *
2015	[BCK15]	$\tilde{O}\left(d\left\|H\right\|_{\max}t\right)$ *
2015	[Ber+15]	$O\left(\frac{N(n+\log N)\log\left(\frac{t}{\Delta t\epsilon}\right)}{\log\log\left(\frac{t}{\Delta t\epsilon}\right)}\right)$ *
2014	[Ber+14]	$\tilde{O}\left(d^2\left\|H\right\|_{\max}t\right)$ *
2013	[BCS13]	$O\left(\left[d^2\left\|H\right\|t+\log\left(\frac{1}{\epsilon}\right)\right]\log^3\left[\frac{dt}{\epsilon}\left(\left\|H\right\|+\left\|H'\right\|\right)\right]n^c\right)$ *
2012	[CW12]	$\tilde{O}\left(N^2\max\left\|h_j\right\|te^{1.6\sqrt{\log(N\max\|h_j\|t)/\epsilon}}\right)$ *
2005	[Ber+05]	$O\left(\left(\min\left\{r\middle\vert\log_2^{(r)}n<2\right\}d^2 5^{2k}\left(d^2\left\|H\right\|t\right)^{1+1/2k}/\epsilon^{1/2k}\right)\right)$ *
2003	[AT03]	$O\left(\frac{tN}{\Delta t}\mathrm{poly}\left(\Delta t,N,n,1/\epsilon\right)\right)$
1996	[Llo96]	$O\left(\mathrm{poly}\left(\frac{1}{\epsilon}\right)\right)$

Table 1.1: In this table we show a number of Hamiltonian simulation algorithms and their performances. The performances that have an * are the query complexity of the algorithm rather than its gate count or circuit depth. In the table above d represents sparsity of the Hamiltonian H, and the algorithms that depend on d assume the Hamiltonian is sparse.

1.3.1 Early Results Using Lie-Trotter-Suzuki Formulae

One of the earliest results in the field of quantum computation was the discovery that local Hamiltonians can be simulated efficiently on a quantum computer [Llo96]. Historically speaking, it showed that the evolution of physical systems, as long as their interactions are local, can be simulated efficiently on a quantum computer, a task which is believed to be hard on a classical computer. The idea in

Seth Lloyd's work comes from an earlier mathematical result [Suz76]: Suppose we are given a Hamiltonian $H = \sum_{j=1}^{N} h_j$, where each h_j is gapped and acts only on a local neighborhood of sites. Therefore we can assume each individual h_j is efficiently simulatable. In order to simulate e^{-iHt} we utilize the following identities:

$$\left(e^{-iAt/k}e^{-iBt/k}\right)^k = e^{-i(A+B)t} + O\left(\frac{t^2}{k}\right) , \tag{1.4}$$

$$\left(e^{-iAt/2k}e^{-iBt/k}e^{-iAt/2k}\right)^k = e^{-i(A+B)t} + O\left(\frac{t^3}{k^2}\right) . \tag{1.5}$$

$$\vdots \tag{1.6}$$

Higher order term have progressively smaller error and they can be systematically produced [HS05; Suz91]. Using a sufficiently high order Lie-Suzuki-Trotter formula and a more careful error analysis yields the results in [Ber+05].

1.3.2 Sparse Hamiltonian Simulation

Another approach that has been pursued to implement Hamiltonian simulation algorithms is to utilize the fact that many physical systems have sparse Hamiltonians. Early results for sparse Hamiltonian simulation relied on a technique called *edge coloring* Fig. 1.2. Effectively, one colors the edges of the Hamiltonian graph of the system in such a way that edges meeting at same vertex have different colors. Each sub-graph represents a 1-sparse Hamiltonian and can be simulated efficiently[Chi+03; AT03; Ber+05; Ber+14]. An early version of this technique is

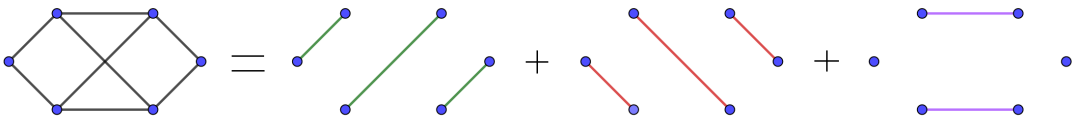

Figure 1.2: (color online) Coloring a Hamiltonian graph into sub-graphs that each can be simulated efficiently.

formally explained in Lemma 1.

Lemma 1 (Decomposition Lemma[AT03, p. 20])**.** *Let H be a row-sparse Hamiltonian over n qubits with at most d non-zero elements in each row. There exists a decomposition of $H = \sum_{j=1}^{N} h_j$, where each h_j is 1-sparse, such that $N = (d+1)^2 n^6$.*

Proof. The proof is constructive: For $(i, j) \in [2^n] \times [2^n]$ and $i < j$ (upper diagonal entries) let the color of each entry (which are represented by edges in the Hamiltonian graph) be labelled by:

$$\text{Color}_H(i,j) = (k, i \text{mod} k, j \text{mod} k, \text{row}_\#(H,i,j), \text{column}_\#(H,i,j)) \ , \tag{1.7}$$

where

- If $i = j$ we set $k = 1$, otherwise it's set as the smallest integer such that $i \not\equiv j (\text{mod} k)$. There is always such a k in the range $[2 \dots n^2]$.
- If $H_{i,j} = 0$, then $\text{row}_\#(H,i,j) = 0$. Otherwise $\text{row}_\#(H,i,j)$ is defined as the index of $H_{i,j}$ in the list of non-zero elements in the i'th row of H. $\text{column}_\#(H,i,j)$ is defined similarly, except rows and columns are switched.
- The coloring is symmetric, so the lower diagonal entries, $\text{Color}_H(i,j) = \text{Color}_H(j,i)$.

Altogether, this method of coloring uses $n^6(d+1)^2$ colors. □

After decomposing the Hamiltonian with regards to Lemma 1, or using more sophisticated coloring schemes (e.g. [Ber+05; Ber+14]), we can use a Lie-Suzuki-Trotter formula, as explained in Sec. 1.3.1 to simulate the Hamiltonian.

1.3.3 Linear Combination of Unitaries

In a seminal paper in 2012, Andrew Childs and Nathan Wiebe introduced another method for simulating Hamiltonians [CW12]. Besides improving the performance of the Hamiltonian simulation algorithm in some asymptotic limits, the fact that it initiated a new paradigm of simulation algorithms is not negligible. That's why in this section we try to give an overview about the core ideas that are involved in this algorithm and the following works that used a similar approach.

Perhaps at the heart of their paper is the observation that if two unitary operators are close to each other, then a linear combination of them can be efficiently implemented on a quantum computer. Although unitary operators are not closed under addition, the linear combinations they end up using in the simulation algorithm are very close to unitary. This means for all practical intents and purposes they are indistinguishable from unitary operators. This observation is formally expressed in Lemma 2:

Lemma 2 (Linear combination of unitaries [CW12, p. 2])**.** *Let $U_a, U_b \in \mathbb{C}^{2^n \times 2^n}$ be unitary operators and let $\Delta = \|U_a - U_b\|$. Then for any $\upsilon \geq 0$, there exists an efficient quantum algorithm that can implement $\upsilon U_a + U_b$ (up to a normalization*

factor) with failure probability $\frac{\Delta^2 \upsilon}{(1+\upsilon)^2} \leq \frac{4\upsilon}{(1+\upsilon)^2}$.

Proof. Let

$$V_\upsilon = \begin{pmatrix} \sqrt{\frac{\upsilon}{\upsilon+1}} & \frac{-1}{\sqrt{\upsilon+1}} \\ \frac{1}{\sqrt{\upsilon+1}} & \sqrt{\frac{\upsilon}{\upsilon+1}} \end{pmatrix} . \tag{1.8}$$

The quantum circuit for implementing the linear combination of U_a and U_b can be seen in Fig. 1.3. The state of the system prior to the measurement is:

$$|0\rangle \left(\frac{\upsilon}{\upsilon+1} U_a + \frac{1}{\upsilon+1} U_b \right) |\psi\rangle + |1\rangle \frac{\sqrt{\upsilon}}{\upsilon+1} (U_b - U_a) |\psi\rangle \ . \tag{1.9}$$

If the outcome of the measurement is 0, then up to normalization factors the circuit has applied the desired linear combination, $|\psi\rangle \mapsto (\upsilon U_a + U_b) |\psi\rangle$. If the measurement reads 1, then the protocol has failed. The failure probability is bounded by:

$$P_+ \leq \frac{\|U_b - U_a\|^2 \upsilon}{(\upsilon+1)^2} = \frac{\Delta^2 \upsilon}{(\upsilon+1)^2} \leq \frac{4\upsilon}{(\upsilon+1)^2} \ . \tag{1.10}$$

□

By applying Lemma 2 recursively they prove the possibility of simulating a general linear combination of unitaries [CW12, Thm. 3]. In order to have a high success probability, there are two conditions required, $\upsilon \gg 1$ and $\Delta \ll 1$. These conditions can be naturally satisfied in a quantum Hamiltonian simulation problem [CW12].

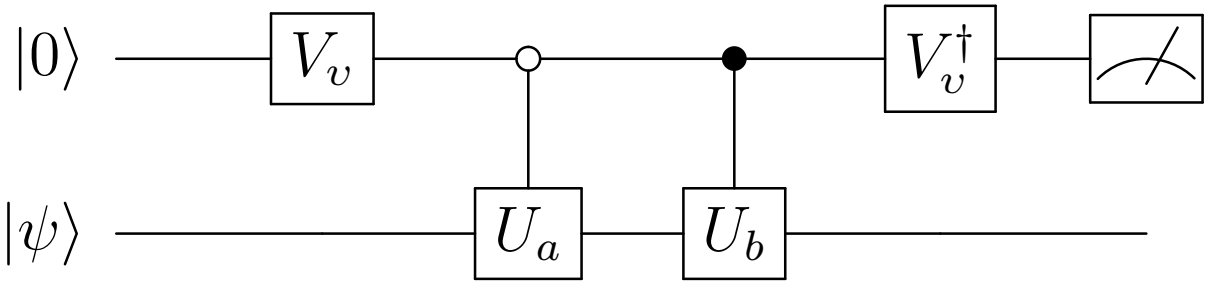

Figure 1.3: The quantum circuit for performing an operator proportional to $\upsilon U_a + U_b$ with probability $1 - \frac{\Delta^2 \upsilon}{(1+\upsilon)^2}$ given a measurement outcome of 0.

1.3.4 Modern Algorithm for Geometrically Local Hamiltonians

In this section I will discuss the core ideas in one of the more recent modern algorithms for simulating geometrically local lattice Hamiltonians [Haa+18]. Before we dive deeper, it is important to know that *local Hamiltonians* are a special case of sparse Hamiltonians. I explained some of the early ideas for sparse Hamiltonian simulation in Sec. 1.3.2. More recent results have saturated the theoretical lower bounds in terms of asymptotic query complexity [LC16b].

Confusingly, the term *local Hamiltonian* is used to describe two distinct types of Hamiltonians in the literature. In order to distinguish them, let us call them *geometrically local* and *non-geometrically local*. A Hamiltonian $H(t)$ is said to be non-geometrically local or k-local if it can be written as a sum of polynomially many terms $H(t) = \sum_{j=1}^{\text{poly}(n)} h_j(t)$, where each $h_j(t)$ acts non-trivially on at most k qubits. A geometrically local Hamiltonian is a subset of k-local Hamiltonians with the condition that each term $h_j(t)$ should act upon k adjacent qubits in some fixed number of spatial Euclidean dimensions.

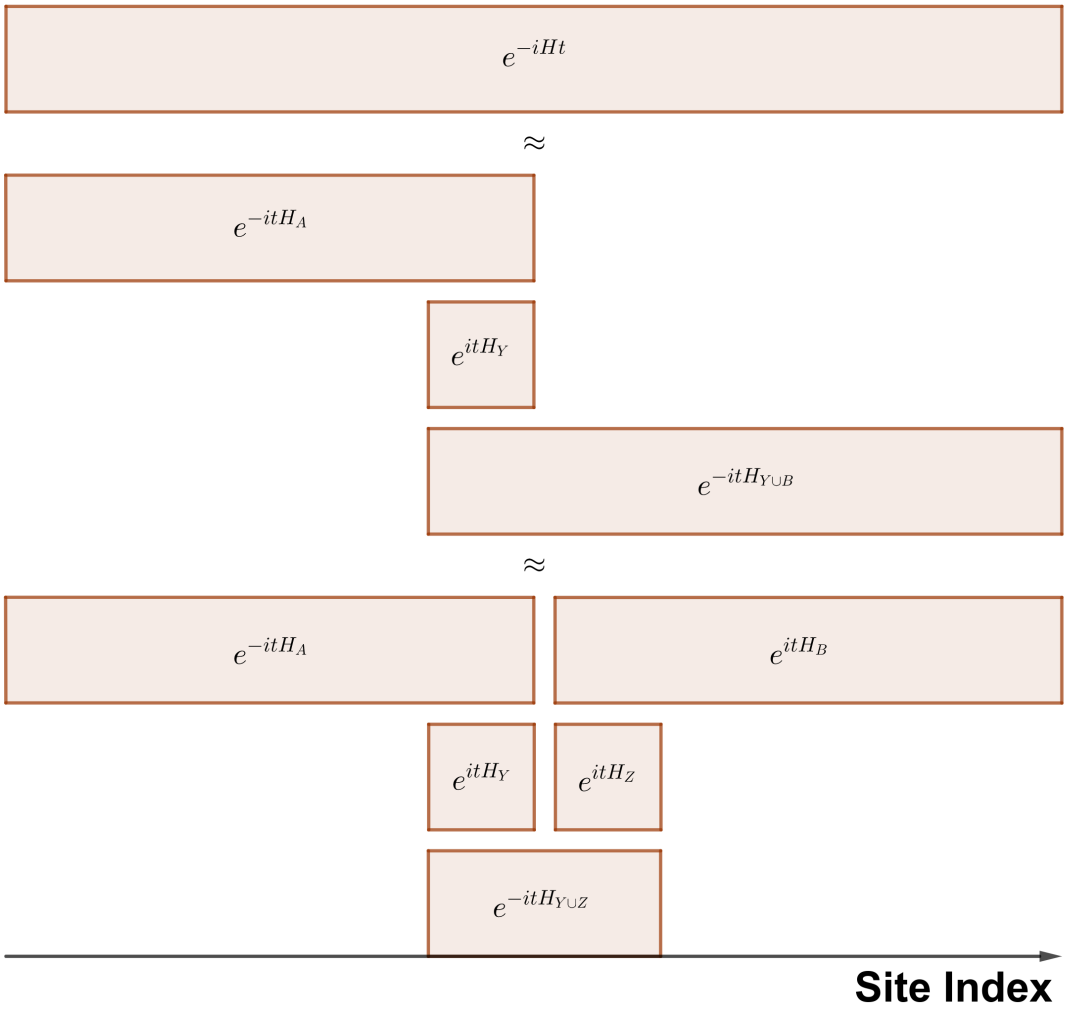

Figure 1.4: How to reconstruct a 1 dimensional local Hamiltonian.

The key idea in [Haa+18] simplifies to the observation that we can write the Hamiltonian evolution as:

$$e^{-itH} \approx \left(e^{-itH_A}\right)\left(e^{+itH_Y}\right)\left(e^{-itH_{Y\cup B}}\right) \ , \tag{1.11}$$

where the regions are sketched in Fig. 1.4. Putting this into words, it means that if we divide our system into two regions, then after applying the unitary evolution operator corresponding to one them, you need to evolve backwards in time around the boundary of the two regions before applying the other unitary evolution operator. The size of region near the boundary is given by a Lieb-Robinson bound [LR72; HK06], which is a function of the so called Lieb-Robinson velocity and the time of evolution. One can repeatedly divide the Hamiltonian into smaller regions until each of the smaller regions becomes easily simulatable.

Theorem 1 states the final result of this approach.

Theorem 1 ([Haa+18, p. 354]). *Let $H(t) = \sum_{X\in\Lambda} h_X(t)$ be a time-dependent Hamiltonian on a lattice Λ of n qubits, embedded in the Euclidean metric space $\mathbb{R}^D$. Let us assume that each unit ball contains $O(1)$ qubits and $h_X = 0$ if $\mathrm{diam}(X) > 1$. Let us also assume that each individual term $h_X(t)$ is efficiently computable and piece-wise and slowly varying on the time domain we want to simulate and has $\|h_X(t)\| \geq 1$ for any value of X and t. Then there exists a quantum algorithm that can approximate the time evolution of H for time t and precision goal ϵ using $O\left(tn\,\mathrm{polylog}(tn/\epsilon)\right)$ local 2-qubit gates and has depth $O\left(t\,\mathrm{polylog}\left(tn/\epsilon\right)\right)$.*

1.4 Simulating Quantum Field theory

Being able to efficiently simulate quantum field theory scattering problems on a universal quantum computer has both theoretical and practical implications. First of all simulating a generic QFT belongs to the BQP-complete complexity class of problems [Jor+18]. If a machine can efficiently simulate generic QFTs, it means that it can solve any problem a universal quantum computer is capable of solving. On the other hand being able to simulate generic complicated QFTs, like the Standard Model efficiently, would immediately help us better understand some aspects of high energy physics. That is why in the past few years there has been a large theoretical and experimental effort for utilizing present quantum devices, also known as noisy intermediate-scale quantum (NISQ) era devices, to simulate simple QFT systems [Klc+18; KS19a; Dav+19; Bañ+19; Sch+19; Cla+18; ANG18; Stu+15; Man+15; Dal+11].

Simulation of a scattering problem in QFT, can be divided into four distinct steps [JLP11; JLP12; JLP14]:

1. Discretize your system and map the remaining degrees of freedom of your system to the degrees of freedom of your quantum computer. On a digital quantum computer this means mapping the degrees of freedom to qubits. This step usually only has to be done once for any type of Hamiltonian and therefore as long as it is efficiently computable, it does not contribute to the overall performance of the algorithm.

2. Initialize your quantum computer so its state represents the initial state of the system you want to simulate. In scattering problems this often means to prepare the vacuum of the theory and then prepare the desired excitations (particles) that will later on interact and scatter.

3. Let the system evolve under the given Hamiltonian for a period of time. This step can be done using an efficient Hamiltonian simulation algorithm, such as the ones I mentioned in Sec. 1.3.

4. Measure the outcome. Reading the outcome of the scattering can be a non-trivial task. In order to make sense of the outcome, one has to do some post-processing on the state, such as adiabatically transforming it to the non-interacting theory or measuring some useful quantum operators using phase estimation.

These steps complete the simulation, however, depending on the type of results one is interested in, some post-processing might be necessary.

1.4.1 Initial State Preparation

Prior to the results demonstrated in Chapters 3 and 4, state preparation has been the slowest part of QFT simulation algorithms [JLP12; JLP14; Klc+18; KS19a]. The reason this was the case is that, Hamiltonian simulation algorithms are often used in the state preparation step of the algorithm as a subroutine, and if one is not careful about their approach to the problems, extra factors would find their way into the performance and make it worse.

Another point that is worth mentioning is that ideally we would like to be able to simulate complicated quantum field theories, such as QCD or the Standard Model. These QFTs have a mixture of fermions and bosons. Keeping that goal in mind, it is imperative to understand that we should start by studying simpler well-understood models, such as the Gross-Neveu model [GN74], ϕ^4-theory or Schwinger model [Sch62], and gradually work our way towards our goal. Perhaps if we had to choose between a fermionic model or a bosonic model to simulate, the easier one would be the fermionic system. The reason for this being the case is that, although fermionic excitations become non-local operators when mapped to qubits [JW28], the non-localities often come in pairs and cancel out [HJ18]. On the other hand Pauli's exclusion principle prohibits fermions from occupying the same quantum numbers. This means that we can very efficiently represent the fermionic operators using qubits. Yet, in order to address bosons we may need a number of qubits per site that is proportional to the cutoff of the theory. That is why in the rest of this manuscript we focus mainly on fermionic systems and leave the bosonic systems for future studies.

One of the most influential results for simulating fermionic quantum field theories is Stephen Jordan, Keith Lee, and John Preskill's paper from 2014, Quantum Algorithms for Fermionic Quantum Field Theories [JLP14]. It showed for the first time that the problem of simulating massive fermionic QFTs can be solved in a time asymptotically proportional to a polynomial function of the parameters of the problem. Specifically, they showcase their algorithm on the Gross-Neveu model, and get total gate counts of $G_{\text{total}} = O(\epsilon^{-8-o(1)})$ as $\epsilon \to 0$, where ϵ is the precision goal

of the algorithm. Because of its importance, we will review the main ideas that are used in the state preparation step of their paper in the following Sec. 1.4.1.1.

1.4.1.1 Jordan-Lee-Preskill

In this section we will discuss how [JLP14] does state preparation in their algorithm. There are four main steps:

1. Start with the non-interacting free theory and prepare the ground state. This means setting the interaction strength, g_0^2, and the nearest-neighbor term to be zero. The ground state of this system can be prepared efficiently because it is a product state.

2. Adiabatically turn on the nearest-neighbor interactions. Originally they proposed doing this step using a high order Lie-Suzuki-Trotter Hamiltonian simulation approach to simulate this step (see Sec. 1.3.1). (By introduction of more efficient Hamiltonian simulation quantum algorithms, such as [CS19; Haa+18] it makes sense to utilize those instead of the outdated Trotter based algorithms.) They show that they need to simulate for $T_{\text{prep}} = O\left(\frac{L^2}{a^4 m^3 \epsilon}\right)$, where L is the system size, a is the lattice spacing, m the physical mass and ϵ is the desired precision we want on the scattering amplitudes. Overall, the number of quantum gates for this step of the algorithm is $G_{\text{prep}} = O\left(\left(\frac{TL}{a^2}\right)^{1+o(1)} \epsilon^{-o(1)}\right) = O\left(\left(\frac{L^3}{a^6 m^3 \epsilon}\right)^{1+o(1)}\right)$.

3. Adiabatically increase the interaction strength while adjusting the m_0 parameter as the physical mass is renormalized. This step require time and gate

count of the same order of the last step.

4. Excite particle wavepackets that have the desired energy and momentum, by introducing a sinusoidal source term to the Hamiltonian. In order to avoid exciting extra particles they needed the source term to be weak compared to the other terms in Hamiltonian. This yielded $G_{\text{excite}=O\left(\epsilon^{-4-o(1)}\right)}$ in the high precision asymptotic limit.

Overall, the slowest parts of the algorithm were the adiabatic steps for preparing the vacuum. In summary the total cost of performing fermionic state preparation using this algorithm would be:

$$G_{\text{total}} = \begin{cases} O\left(\epsilon^{-8-o(1)}\right), & \text{as } \epsilon \to 0 \ , \\ O\left(p^{9+o(1)}\right), & \text{as } p \to \infty \ . \end{cases} \tag{1.12}$$

This result is significant because it shows that simulating fermionic QFTs is in the class of polynomially solvable problems on a quantum computer (also known as BQP). Despite its theoretical relevance, because of these very large powers, it is unlikely that this exact algorithm will be practically implemented. However, there is a silver-lining here too; in many cases when the performance of an algorithm is too slow compared to what people intuitively expect, there is some room for improvement. And as we shall see in Chapters 3 and 4 it happens that there are indeed more efficient ways of preparing initial states of a fermionic QFT.

Chapter 2: Preliminary Tools

2.1 Overview

In this chapter we will discuss some of the tools that will be utilized in Chapters 3 and 4. First in Sec. 2.2 we discuss the phase estimation algorithm. This is a key sub-routine in many of the algorithms discussed in this manuscript. Then, in Sec. 2.3 we will discuss the Gross-Neveu model, which is a fermionic QFT designed to imitate some features of QCD.

2.2 Phase Estimation Algorithm

The phase estimation algorithm was introduced in 1995 by Alexei Kitaev [Kit95]. Inspired by [NC00], we will fisrt state the problem and then give the algorithm that solves it and analyze its performance. Then we will discuss a more recent result with tight asymptotic dependencies based on [SHF14] and compare the two algorithms.

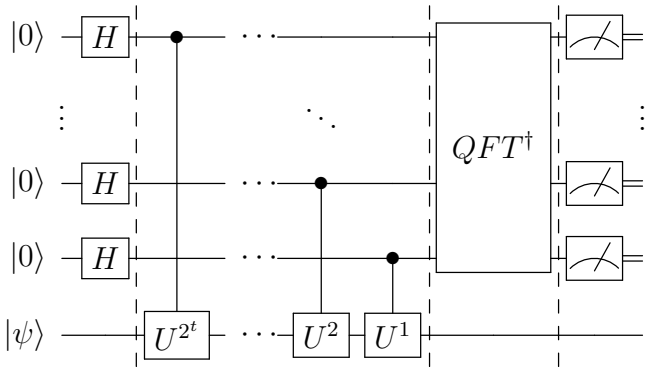

Figure 2.1: Quantum circuit for phase estimation.

2.2.1 Statement of the Problem

Given a unitary operator U that acts upon m qubits and an eigenstate $|\psi\rangle$, such that $U|\psi\rangle = e^{2\pi i\theta}|\psi\rangle$, find θ. The problem assumes having access to oracle calls to Controlled$-U^{2^j}$ unitary operators, where U^{2^j} are different powers of the unitary matrix U.

2.2.2 Normal Phase Estimation

Let's analyze the circuit in Fig. 2.1. The ancilla qubits start in the standard $|0\rangle$ state. We then apply a Hadamard gate on each ancilla qubit. The state of the system at the end of this stage is given by:

$$(|+\rangle)^{\otimes t}|\psi\rangle \tag{2.1}$$

The state in the second register is an eigenstate of all of the operators in the circuit and remains uninterrupted throughout the entire algorithm. Therefore we

omit the second register in the following equations and focus mainly on the state of the qubits in the qubits in the first register. After applying the controleld unitaries the state of the first register is going to be:

$$\frac{1}{2^{t/2}}\left(|0\rangle + e^{2^t \pi i\theta}|1\rangle\right)\ldots\left(|0\rangle + e^{2^2\pi i\theta}|1\rangle\right)\left(|0\rangle + e^{2\pi i\theta}|1\rangle\right) \tag{2.2}$$

$$= \frac{1}{2^{t/2}}\left(|0\rangle + e^{2\pi i\left(2^{t-1}\theta\right)}|1\rangle\right)\ldots\left(|0\rangle + e^{2\pi i\left(2^1\theta\right)}|1\rangle\right)\left(|0\rangle + e^{2\pi i\left(2^0\theta\right)}|1\rangle\right) \tag{2.3}$$

$$= \frac{1}{2^{t/2}}\sum_{k=0}^{2^t-1} e^{2\pi ik\theta}|\bar{k}\rangle\ , \tag{2.4}$$

where the bar in $|\bar{k}\rangle$ means that each digit in the binary representation of k has been mapped to a qubit. After applying the inverse quantum Fourier transform the state is going to be:

$$\frac{1}{2^{t/2}}\sum_{k=0}^{2^t-1} e^{2\pi ik\theta}\left(\frac{1}{2^{t/2}}\sum_{j=0}^{2^t-1} e^{-2\pi ijk/2^t}|j\rangle\right) \tag{2.5}$$

$$= \frac{1}{2^t}\sum_{j,k=0}^{2^t-1} e^{2\pi ik\left(\theta-\frac{j}{2^t}\right)}|j\rangle \tag{2.6}$$

$$= |\overline{2^t\theta}\rangle \tag{2.7}$$

$$= |\theta_1\rangle|\theta_2\rangle\ldots|\theta_t\rangle\ , \tag{2.8}$$

where in Eq. (2.7), we assume the phase θ can be exactly represented with t binary digits, $\bar{\theta} = 0.\overline{\theta_1\theta_2\ldots\theta_t}$. This means that if we measure the first register of the system in the standard basis, it precisely outputs the digits of the phase θ. If we cannot exactly represent θ using n binary digits but only approximate it, then it turns out one needs $\left\lceil \log\left(2+\frac{1}{2\epsilon}\right)\right\rceil$ extra qubits in the first register to be able to get the best

n-digit approximation of θ with success probability $1 - \epsilon$ [NC00, Section 5.2.1].

The Inverse Fourier transformation at the end can be efficiently done with a number of gates proportional to $O(t \log t)$. Overall this makes the algorithm to have a runtime of:

$$O\left(\left(n + \left\lceil \log\left(2 + \frac{1}{2\epsilon}\right)\right\rceil\right) \log\left(n + \left\lceil \log\left(2 + \frac{1}{2\epsilon}\right)\right\rceil\right)\right) = \tilde{O}\left(n \log n\right) , \quad (2.9)$$

plus the number of gates required to efficiently apply the controlled-U^j gates.

2.2.3 Faster Phase Estimation

2.3 The Gross-Neveu Model

Chapter 3: Faster quantum algorithm to simulate Fermionic quantum field theory

3.1 abstract

In quantum algorithms discovered so far for simulating scattering processes in quantum field theories, state preparation is the slowest step. We present an algorithm for preparing particle states to use in simulation of Fermionic Quantum Field Theory (QFT) on a quantum computer, which is based on the matrix product state ansatz. We apply this to the massive Gross-Neveu model in one spatial dimension to illustrate the algorithm, but we believe the same algorithm with slight modifications can be used to simulate any one-dimensional massive fermionic QFT. In the case where the number of particle species is 1, our algorithm can prepare particle states using $O\left(\epsilon^{-3.23\ldots}\right)$ gates, which is much faster than previous known results, namely $O\left(\epsilon^{-8-o(1)}\right)$. Furthermore, unlike previous methods which were based on adiabatic state preparation, the method given here should be able to simulate quantum phases unconnected to the free theory.

3.2 Introduction

Here we analyze the simulation of fermionic quantum field theory (QFT) models on a quantum computer. We use massive Gross-Neveu model to illustrate the procedure. However, the procedures are quite general and can be used to simulate other fermionic systems too. The simulation consists of initializing the incoming particle states on our quantum computer, simulating unitary time evolution according to the lattice quantum field theory Hamiltonian, and then measuring appropriate observables to extract scattering cross sections. Here we focus exclusively on the state preparation step of the algorithm, because it has been the bottleneck of previous quantum algorithms for simulating scattering in quantum field theories [JLP12; JLP14; JLP11].

The original Gross-Neveu model is a relativistic and renormalizable quantum field theory of N species of fermions in $(1+1)$ space-time dimensions. It is a rich theory and shares many interesting features with quantum chromodynamics (QCD), *e.g.,* asymptotic freedom and dimensional transmutation [GN74].

Our algorithm simulates scattering of fermionic particles in the Gross-Neveu quantum field theory with a mass term. The mass term ensures that the theory is gapped, *i.e.,* that there is a nonzero energy difference between the ground state and first excited state in the infinite volume limit. This allows us to construct the vacuum (ground state) efficiently by classically computing a Matrix Product State (MPS) description of the vacuum state and then compiling that description directly into a quantum circuit for preparing that state. We then use Rabi oscillations to

efficiently excite single-particle wave packets. This completes the state preparation phase of the simulation, after which the scattering of the particles off each other can be simulated using high order Suzuki-Trotter formulas exactly as in [JLP14] or using more recent results for lattice Hamiltonian simulation as in [Haa+18]. Relative to the previous state of the art [JLP14] our state preparation method has better asymptotic complexity in the limit of high precision and is able to simulate the symmetry-broken phase of the Gross-Neveu model, which was inaccessible to prior state preparation methods, which simulated an adiabatic process starting from the free theory.

3.3 Overview

3.3.1 Gross Neveu Model

The original Gross-Neveu theory was a QFT describing fermions in $(1+1)$ space-time dimensions, introduced by Gross and Neveu in 1974 [GN74] as a toy model for QCD. The theory has many interesting features; *e.g.,* similar to QCD, it has asymptotic freedom [GN74]. Here, as in [JLP14], we consider a variant of the Gross-Neveu model in which the Lagrangian density includes an explicit mass term. Specifically,

$$\mathcal{L} = \sum_{j=1}^{N} \bar{\psi}_j \left(i\partial\!\!\!/ - m_0 \right) \psi^j + \frac{g^2}{2N} \left(\sum_{j=1}^{N} \bar{\psi}_j \psi^j \right)^2 , \tag{3.1}$$

where each field $\psi_j(x)$ is a two-component spinor, $\partial\!\!\!/ = \sum_\mu \gamma^\mu \partial_\mu$ where γ_μ are the 2D Dirac matrices, m_0 is the bare mass of the model, g is the coupling constant,

and $\bar{\psi} = \psi^\dagger \gamma^0$. Outside of high energy physics, this model also has been used in different branches of condensed matter physics, such as conducting polymers and systems of strongly correlated electrons [LBF98; TU05a; TU05b].

One can verify that Eq. (3.1) is invariant under Lorentz transformations. Assuming $m_0 > 0$, the theory has a gap between vacuum and a single particle state. Lorentz-invariance will guarantee the spectrum to be continuous above the first excitation. However, this symmetry and therefore the continuous spectrum are violated when the theory is discretized. Despite this, as discussed in [JLP14], one can achieve any desired accuracy by using a sufficiently fine lattice spacing.

Another effect of discretizing the space-time and putting our system on a lattice would be doubling of species of Dirac fermions, or the so-called "Fermion doubling" problem [NN81b]. For theories with chiral symmetry, such as the massless Gross-Neveu model, there is no way to keep the action real, local and free on a lattice and preserve translational invariance without getting the extra fermions [NN81a]. However, the mass term breaks chiral symmetry and we can therefore safely solve the fermion doubling problem in the massive case by adding a term to the Hamiltonian, known as the Wilson term, which decouples the extra fermions by giving them large mass [Wil74].

3.3.2 Performance

In order to simulate the scattering process on a digital quantum computer, we first put our system on a spatial lattice of length L and lattice spacing a with periodic

boundary conditions. We then start the algorithm by preparing the ground state of the resulting lattice quantum field theory described by the discretized version of Eq. (3.1). There are efficient classical algorithms for finding the ground state of one dimensional gapped Hamiltonians as an MPS. There are rigorous upper bounds for the performance of classical algorithms to find the MPS [Hua14; Ara+17], which are not necessarily applicable to our case (because the norms of individual local terms in the Hamiltonian grow indefinitely as you shrink the lattice spacing a). For the purpose of this paper we use classical numerical heuristics such as Density Matrix Renormalization Group (DMRG), that in practice run in linear time in the number of sites. Specifically the runtime of DMRG in practice is $O\left(n\chi^3\right)$; where χ is the bond dimension of the matrix product state [Sch05; Sch11; Whi92]. Physical arguments show [Swi13; OHA99] that it should suffice to take bond dimension

$$\chi = ke^{S_{1/2}} \ , \tag{3.2}$$

where $S_{1/2}$ is the entanglement entropy between the two half-spaces of the state being prepared, and errors decrease superpolynomially as we increase k beyond unity. For the Gross-Neveu model we can first consider the non-interacting ($g = 0$) case, in which the theory splits into N copies of a Dirac quantum field theory. We thus have for the Gross-Neveu entropy $S^{\mathrm{GN}}(g)$:

$$S^{\mathrm{GN}}_{1/2}(g = 0) = N S^{\mathrm{Dirac}}_{1/2}. \tag{3.3}$$

We are interested in asymptotically high precision. This is the limit where the correlation length $1/m$ is much longer than the lattice spacing a. In this limit we obtain the entropy from the conformal field theory describing the massless fermion in one spatial dimension, namely [Swi13; OHA99; CH09; Gin88; Qua15]

$$S_{1/2}^{\text{Dirac}} \simeq \frac{c}{6} \log\left(\frac{1}{ma}\right) \qquad (ma \ll 1) \tag{3.4}$$

where $c = 1$ is the central charge. (In the possibly more familiar case of a line segment rather than a half-space one would have twice the entanglement entropy: $\frac{c}{3} \log\left(\frac{1}{ma}\right)$.) Thus, we have

$$\chi = k e^{N S_{1/2}^{\text{Dirac}}} \tag{3.5}$$

$$= k \left(\frac{1}{ma}\right)^{N/6}. \tag{3.6}$$

The analysis of [JLP14] shows that the discretization errors scale as $\epsilon \sim a$. Thus,

$$\chi \sim k \epsilon^{-N/6}. \tag{3.7}$$

The relationship between k and error can be understood using the results of [Swi13]. Consider Lorentz-invariant 1+1 dimensional quantum field theory discretized onto a lattice of spacing a. Let $\lambda_1 \geq \lambda_2 \geq \lambda_3 \ldots$ be the eigenvalues of the reduced density matrix if we divide the vacuum into two halves. In other words, $\lambda_1, \lambda_2, \ldots$ are the Schmidt coefficients in order of decreasing magnitude if we do a Schmidt

decomposition of the vacuum state. Then, as shown in [Swi13],

$$f(\chi) \equiv \sum_{j=\chi+1}^{\infty} \lambda_j \sim \exp\left[-\frac{(\ln\chi - S_{1/2})^2}{2S_{1/2}}\right] \tag{3.8}$$

for χ large (*i.e.* $\chi > e^{S_{1/2}}$). The magnitude of the error, as measured by trace distance, that we incur by truncating the Schmidt decomposition to some finite bond dimension χ is captured by $f(\chi)$. From Eq. (3.8) one sees that $f(\chi) = \epsilon$ is achieved by choosing $\chi = ke^{S_{1/2}}$ with

$$\begin{aligned} k &= \exp\left[\sqrt{2S_{1/2}\ln(1/\epsilon)}\right] && (3.9)\\ &= \exp\left[\sqrt{\frac{N}{3}\ln\left(\frac{1}{ma}\right)\ln\left(\frac{1}{\epsilon}\right)}\right] && (3.10)\\ &\sim \epsilon^{-\sqrt{N/3}}. && (3.11) \end{aligned}$$

where the last line follows from $a \sim \epsilon$. Combining Eq. (3.7) and Sec. 3.3.2 thus yields

$$\chi = O(\epsilon^{-N/6-\sqrt{N/3}}). \tag{3.12}$$

The classical pre-computation step using DMRG takes time of order $n\chi^3$, where n is the number of lattice sites. Therefore, the complexity of this step is:

$$\begin{aligned} C_{\text{DMRG}} &= O\left(n\epsilon^{-N/2-\sqrt{3N}}\right) && (3.13)\\ &= O\left(\epsilon^{-N/2-1-\sqrt{3N}}\right), && (3.14) \end{aligned}$$

where the last line follows from $n = L/a$ and $a \sim \epsilon$. As shown in subsequent

sections, the quantum state preparation circuit uses $O(\epsilon^{-3-o(1)})$ gates. Thus, the classical preprocessing step is the dominant cost. In particular, for $N = 1$ the cost is $O(\epsilon^{-3.23...})$.

An MPS can be compiled into a quantum algorithm for preparing it using Singular Value Decomposition (SVD). The idea is to bring the MPS into a standard form, where each matrix is an isometry that maps the left virtual index to the right virtual index and the physical index. The corresponding quantum circuit applies these isometries one by one on the qubits, until you have the full MPS state. The overall classical subroutine for SVD on the matrices of our system runs in a polynomial time less than $n\chi^3$. Applying these quantum isometries on our system would need at most $O\left(n\chi^2\right)$ gates, therefore, this step is not going to be the leading term in the overall performance of the algorithm [Sch+07; Sch+05].

After preparing the vacuum, the next step is to excite particle states. By introducing sinusoidal source terms in the Hamiltonian, we induce Rabi oscillations to excite two particle wave packets with desired energy and momenta with success probabilities close to 1. Specifically in Sec. 3.5, we show that we can prepare a particle state of the interacting theory in time $\frac{\pi}{\lambda}$, with probability

$$P = 1 - O\left(\frac{\lambda}{\delta} - \left(\frac{\lambda}{\omega}\right)^2\right), \tag{3.15}$$

where λ indicates the strength of the source term, δ is the minimum detuning to higher excited states, and ω is the energy of the particle compared to the vacuum. According to Eq. (3.15), $\frac{\lambda}{\delta}$ is proportional to $1-P$, the chance of failure. We set this

to ϵ, which is sufficient to achieve order ϵ relative error in estimates of scattering cross sections, as defined below in Eq. (3.17). After the particles are prepared we turn off the source term and let them interact under the Hamiltonian for a desired time. The simulation of the Hamiltonians can be done using a high order Suzuki-Trotter expansion.

Detailed analysis [Haa+18; JLP14] shows that by doing a high order Suzuki-Trotter expansion the simulation of our Hamiltonian would require number of gates scaling as:

$$G = O\left(\left(\frac{TL}{a^2}\right)^{1+o(1)} \epsilon^{-o(1)}\right) \ , \tag{3.16}$$

where T is the total time we want to simulate and ϵ represents the desired precision of the calculated scattering amplitude; *i.e.* if the discretized algorithm outputs scattering amplitude σ' while the actual cross section amplitude of the scattering is σ, then:

$$(1-\epsilon)\,\sigma \leq \sigma' \leq (1+\epsilon)\,\sigma \ . \tag{3.17}$$

So, if the time required to excite a particle is $\frac{\pi}{\lambda}$, then the number of gates required to prepare the initial particles would scale as:

$$G_{\text{prep}} \ = O\left(\left(\tfrac{L}{a^2\lambda}\right)^{1+o(1)} \epsilon^{-o(1)}\right) \tag{3.18}$$

For high precision results we need a to be proportional to ϵ, so the overall cost of

state preparation would scale as:

$$G_{\text{prep}} = O\left(\epsilon^{-3-o(1)}\right) \ . \tag{3.19}$$

This is asymptotically smaller than the complexity of the classical DMRG preprocessing step. Therefore, the overall performance of this algorithm is limited by the classical part of it, $O\left(\epsilon^{-3.23\ldots}\right)$. This is much better than the previous result in [JLP14], $O\left(\epsilon^{-8-o(1)}\right)$. To simulate the interaction, we now turn off the source term in the Hamiltonian and use a similar Suzuki-Trotter expansion to simulate it. The performance of this part of the algorithm is also given by Eq. (3.16). After we simulate the scattering of the particles we can read the outcome by the phase estimation algorithm, that is explained in [JLP14].

3.4 Preparing Matrix Product State of the Ground State of the Interacting Hamiltonian

We can use Jordan-Wigner transformation to map our fermionic system to spins [JW28]. Then we can see if our spin Hamiltonian is local. We also know that there exists a mass gap for the theory. If the $(1+1)$-dimensional Hamiltonian is local and gapped, then we know the ground state obeys an area law[Has07; VMV13]. This in turn guarantees existence of a matrix product state representation with low bond dimension [Vid04].

To simulate the system on a quantum computer we discretize space onto a one-

dimensional lattice of spacing a. Including the Wilson term the resulting discretized version of the massive Gross-Neveu model is given by the following Hamiltonian.

$$H = H_0 + H_g + H_W \,, \tag{3.20}$$

where

$$H_0 = \sum_{x\in\Omega} a \sum_{j=1}^{N} \sum_{\alpha,\beta\in\{0,1\}} \bar{\psi}_{j,\alpha}(x) \left[-i\gamma^1_{\alpha\beta} \frac{\psi_{j,\beta}(x+a) - \psi_{j,\beta}(x-a)}{2a} + m_0 \delta_{\alpha,\beta} \psi_{j,\beta}(x) \right] , \tag{3.21}$$

$$H_g = -\frac{g_0^2}{2} \sum_{x\in\Omega} a \left(\sum_{j=1}^{N} \sum_{\alpha\in\{0,1\}} \bar{\psi}_{j,\alpha}(x) \psi_{j,\alpha}(x) \right)^2 , \tag{3.22}$$

$$H_W = \sum_{x\in\Omega} a \sum_{j=1}^{N} \sum_{\alpha\in\{0,1\}} \left[-\frac{r}{2a} \bar{\psi}_{j,\alpha}(x) \left(\psi_{j,\alpha}(x+a) - 2\psi_{j,\alpha}(x) + \psi_{j,\alpha}(x-a) \right) \right] . \tag{3.23}$$

Here, H_g is the interaction term, and H_W is the Wilson term, $1 \leq j \leq N$ indicates the Fermion species and $0 < r \leq 1$ is called the Wilson parameter. H is spatially local in the sense that it consists only of single-site and nearest-neighbor terms on the lattice.

All of these Hamiltonian terms consist of pairs of $\bar{\psi}\psi$ terms, and as shown in Sec. 3.7, the Jordan-Wigner transformation yields local spin terms. Also, the massive Gross-Neveu model is gapped, therefore the ground state of this theory obeys area law [Has07]. Therefore, as discussed in Sec. 3.3.2 we can find an MPS representation of the ground state in polynomial runtime. However, if we are will-

ing to repeat the simulation to reduce the statistical uncertainty, finding the MPS representation would be a one-time cost and we don't have to repeat it every time we run the quantum part of the simulation. On the other hand, if we change any of the parameters, *e.g.* even the lattice spacing, we will have to repeat this procedure [Hua14].

3.5 Exciting the state using Rabi oscillations

After preparing the vacuum state using matrix product states, the next step is to prepare initial wave packets. We propose doing this by simulating the application of an oscillating perturbation to the Hamiltonian which is on resonance for the creation of a single particle. We do this in two widely separated locations to prepare a pair of wave packets representing particles of high momentum on a collision course. In broad terms, this is the same procedure proposed in the prior algorithm of [JLP14]. However, our analysis here is nonperturbative and consequently achieves tighter error bounds as a function of the strength of the driving term. We can thus improve the complexity of the algorithm by driving the transition more rapidly while maintaining good upper bounds on error.

In more detail, we propose simulating the dynamics induced by

$$H(t) = H_0 + \lambda \cos(\omega t) W \tag{3.24}$$

where

$$W = \int dx \left(f(x)\psi_{i,\alpha}(x) + f^*(x)\psi^\dagger_{i,\alpha}(x) \right) \tag{3.25}$$

and H_0 is the unperturbed Gross-Neveu Hamiltonian. Here, i and α are chosen according to the desired type of particle and $f(x)$ is an envelope function that selects the wave packet's location and momentum. For example, $f(x)$ could be taken to be a Gaussian: $f(x) \propto e^{ipx - x^2/\sigma^2}$. As explained in [JLP14], choosing an appropriate form of this envelope function f selects wave packet states with the desired momentum.

The driving frequency ω is taken to be on-resonance with the desired transition. If the wave packet is sufficiently broad spatially, and hence narrow in momentum space, then it has a relatively sharply defined energy of $\sqrt{p^2 + m^2}$, which we use as our driving frequency ω. Our choice of $f(x)$ ensures that the matrix elements of W coupling to momenta outside the momentum space support of the wave packet are exponentially suppressed. Thus, the main source of error is the possibility of creating the wrong number of particles. The operator W has zero matrix element to create states with even numbers of particles. Thus, the nearest-to-resonance state that can be excited by W is the state of three particles each with momentum $p/3$. The energy of this state is $3\sqrt{(p/3)^2 + m^2}$, which in the ultrarelativistic limit ($p \gg m$) exceeds the energy of the desired state ($\sqrt{p^2 + m^2}$) by $4m^2/p$. The theory of Rabi oscillations shows that if we choose the strength of our driving term λ sufficiently small compared to the strength of this detuning $\delta = 4m^2/p$ the probability of exciting this three-particle state can be arbitrarily suppressed. In the following

subsections, Sec. 3.5.1 and Sec. 3.5.2, we make this quantitative. The end result is that the success probability obeys

$$P = 1 - O\left(\lambda/\delta + \lambda^2 t/\delta + \lambda^2/\omega^2\right). \tag{3.26}$$

The Rabi rotation from the vacuum to the desired one-particle state takes time $t = \pi/\lambda$. Thus,

$$P = 1 - O\left(\lambda/\delta + \lambda^2/\omega^2\right). \tag{3.27}$$

To achieve success probability $P = 1-\epsilon$ by simulating this state preparation process using high order Suzuki-Trotter formulae yields a total complexity of $O(\epsilon^{-3-o(1)})$ as discussed in Sec. 3.3.2.

In the next two subsections, Sec. 3.5.1 and Sec. 3.5.2 we bound the error we make when we prepare our particles with this algorithm, and show that we can prepare particles with probabilities close to 1. There are two ingredients to this proof, first in Sec. 3.5.1 we bound the error we make when we assume our system to be a 2-level system. Then in subsection Sec. 3.5.2, we analyze the resulting 2-level system using Floquet's Theorem to calculate the probability of successfully exciting one particle.

As explained in [JLP14], there are two type of failures for the state preparation algorithm. If either or both of the incoming particles are not created, this can be detected by the final measurements of the simulation. The probabilities of exciting zero or more than one particles are suppressed and the following theorems put

bounds on them. The latter contributes to the overall precision of the algorithm, ϵ, and it can be controlled by tuning λ.

We note that our analysis is not fully rigorous in the following sense. To avoid extra technical complexity in Secs. 3.5.1 and 3.5.2 we make two simplifying assumptions. First, we consider the creation of eigenstates rather than wave packets. This can be justified by choosing wave packets whose energy uncertainty is small compared to the inverse duration of the excitation process. Second, in section Sec. 3.5.2 we make the simplifying assumption that the energy levels that we drive a transition between are each nondegenerate and furthermore that the driving operator is purely off-diagonal. In actuality, the excited state we are targeting at momentum p is degenerate with a momentum $-p$ state. However, our choice of envelope function f ensures that matrix elements of the perturbation which couple to the momentum $-p$ state can be exponentially suppressed. Thus, we believe the additional complications associated with a fully realistic treatment do not change the overall scaling. Granting the simplifying assumptions as given, our analysis of the resulting simplified model is fully rigorous.

3.5.1 Few-level Approximation

In order to estimate and bound the probability to successfully excite a single particle state, we use two approximations. First in this section we look into what is known as the few-level or 2-level approximation and bound the error occurring from this approximation. In the next subsection we look into the rotating wave

approximation by using an analytical approximate solution to the 2-level driven system. To avoid inconvenience associated with tracking irrelevant global phases we work with density matrices rather than state vectors. However, the dynamics is closed-system and all states remain pure.

Theorem 2. *Assume we have a Hamiltonian* $H_0 + \lambda \cos(\omega t) W$ *with* $\|W\| = 1$. *Let* $\rho(t)$ *be the projector onto the state obtained at time* t *starting with the ground state of* H_0 *at* $t = 0$. *Let* $\rho^{(-)}$ *be the projector onto the state at time* t *obtained by projecting* $H_0 + \lambda \cos(\omega t) W$ *onto the span of the lowest* ν *eigenstates of* H_0 *and solving the resulting Schrodinger equation in this* ν*-dimensional Hilbert space. Then:*

$$\left|\mathbf{Tr}\left[\rho^{(-)}(t)\,\rho(t)\right]\right| \geq 1 - \left(2\nu\lambda + 3\nu\lambda^2 t\right)\frac{1}{\delta}\,, \tag{3.28}$$

where δ *is the minimum detuning from one of the other excited states (*i.e. *minimum energy distance between* $\{E_0+\omega, \ldots, E_{\nu-1}+\omega\}$ *and the rest of the spectrum of* H_0*).*

From Eq. (3.28) it is evident that smaller values of ν and larger values of δ mean a better approximation. For the purpose of this paper ν is degeneracy of the ground state in the rotating frame, or in other words the number of states that are on-resonance with it. For an anharmonic system with mirror symmetry between right-going and left-going particles we would have $\nu = 3$. However, with our choice of the envelope function in Eq. (3.25), we can effectively break this reflection symmetry of the Hamiltonian and get $\nu = 2$. A proof for this theorem is given in Sec. 3.8.

3.5.2 Floquet's Theorem applied to Rabi Oscillations

In the last subsection we bounded the error incurred by treating the system as a 2-level system. Within the 2-level approximation we analyze the dynamics using Floquet theory, following the treatment of Deng *et al.* [Den+16]. We thus obtain an upper bound on the probability of remaining in the ground state of the 2-level system. By adding these two sources of error we obtain a bound on total error.

The main ingredient in Deng *et al.* analysis is Floquet's Theorem, which states that if you have a periodic Hamiltonian in time, there exists a simple change of basis so the eigenstates have the same periodicity [Flo83]. Floquet's theorem is well studied and is used in a variety of contexts. For example see [BJL92; CL99; Mic+07] and references therein. Using Floquet's theorem we prove the following error bound.

Theorem 3. *Assume we have a 2-level Hamiltonian:*

$$H = -\frac{\Delta}{2}\mathbb{Z} + \lambda \cos(\omega t)\mathbb{X} \ , \tag{3.29}$$

where $\mathbb{X}$ *and* $\mathbb{Z}$ *are Pauli matrices and* $\Delta > 0$ *is a real number. We initialize our state at time* $t = 0$ *to be* $|0\rangle$ *in the standard basis. For* $\lambda \ll \omega$*, after time* $t = \frac{\pi}{\lambda}$*,*

$$\left|\left\langle 1 \left| \psi\left(\frac{\pi}{\lambda}\right)\right\rangle\right| \geq 1 - \frac{1}{\sqrt{3}}\left(\frac{\lambda}{\omega}\right)^2 - O\left(\left(\frac{\lambda}{\omega}\right)^4\right) \ . \tag{3.30}$$

A proof for this theorem is presented in Sec. 3.9.

3.5.3 Total Error

Theorem 2 shows that the squared inner product between the exact state produced and the state calculated in the 2-level approximation is at least $1-2\epsilon_1$, where $2\epsilon_1 = 4\lambda+6\lambda^2 t/\delta$. Hence, up to higher order corrections, the inner product between the exact state produced and the state calculated in the 2-level approximation is $1-\epsilon_1$. Theorem 3 shows that the inner product between the state predicted within the 2-level approximation and the desired final state is at least $1-\epsilon_2$, where (neglecting higher order corrections) $\epsilon_2 = \frac{1}{\sqrt{3}}\lambda^2/\omega^2$. Therefore, the inner product between the exact state produced and the desired state is at least $1-\epsilon_1-\epsilon_2-2\sqrt{\epsilon_1\epsilon_2}$. We can simplify this expression by noting that $\sqrt{\epsilon_1\epsilon_2} \leq \max\{\epsilon_1, \epsilon_2\}$. So, the inner product between the exact state obtained and the desired state is $1 - O(\epsilon_1 + \epsilon_2)$, and the probability of success, which is the square of this inner product is also $1-O(\epsilon_1+\epsilon_2)$. This yields Eq. (3.26) and Eq. (3.15).

3.6 Energy and Momentum

After preparing the vacuum of the interacting theory using MPS, we follow a procedure explained in [JLP14]; only a short summary of this procedure is included here. By using sinusoidal source terms in the Hamiltonian, we drive our system to excite a specific energy and momentum. Non-momentum preserving excitations can be neglected because our choice of envelope function f ensures that they have exponentially suppressed matrix elements [JLP14].

The renormalized mass m is no longer equal to the bare mass m_0 in the in-

teracting theory; it's a nontrivial function of bare mass m_0, interaction strength g_0 and lattice spacing a. To know what frequency, ω, to use to excite particles it is necessary to know the renormalized mass m . Despite its nontrivial form, in many instances it can be calculated using perturbation theory (as has been done in [JLP11; JLP14]). The other approach would be to try and excite a single particle using guess values of m in the same order of m_0; then one can use phase estimation algorithms to check whether they succeeded in exciting a particle and what is the actual mass of it. For a specific setup of initial conditions and lattice spacing this would be a one-time cost. In particular, if one intends to run the algorithm many times for statistical precision, this cost is incurred only once.

3.7 Locality Of The Equivalent Spin Hamiltonian

Here we will use Jordan-Wigner transformation and derive the mapped Hamiltonian terms explicitly. Fermionic systems obey anti-commutation relations that cause the states to be non-local.

$$\left\{\psi_{j,\alpha}(x), \psi^{\dagger}_{k,\beta}(y)\right\} = a^{-1}\delta_{j,k}\delta_{\alpha,\beta}\delta_{x,y}\mathbb{I}, \tag{3.31}$$

$$\left\{\psi^{\dagger}_{j,\alpha}(x), \psi^{\dagger}_{k,\beta}(y)\right\} = \{\psi_{j,\alpha}(x), \psi_{k,\beta}(y)\} = 0, \tag{3.32}$$

where $\delta_{m,n}$ is the Kronecker Delta function, j and k represent different Fermion species and α and β indicate matter and antimatter particles. The Jordan-Wigner

transformation is defined as:

$$\psi_{j,0}\left(\eta a\right)$$
$$\rightarrow \frac{-1}{\sqrt{a}} \bigotimes_{\kappa=1}^{\eta-1} \left(\bigotimes_{\xi=1}^{N} \left(\mathbb{Z}_{(j,0)}^{(\kappa)} \otimes \mathbb{Z}_{(j,1)}^{(\kappa)} \right) \right) \otimes \bigotimes_{\xi=1}^{j-1} \left(\mathbb{Z}_{(j,0)}^{(\eta)} \otimes \mathbb{Z}_{(j,1)}^{(\eta)} \right) \otimes \left(a^{+} \right)_{(j,0)}^{(\eta)} \otimes \mathbb{I}_{(j,1)}^{(\eta)} \ , \tag{3.33}$$

$$\psi_{j,1}\left(\eta a\right)$$
$$\rightarrow \frac{-1}{\sqrt{a}} \bigotimes_{\kappa=1}^{\eta-1} \left(\bigotimes_{\xi=1}^{N} \left(\mathbb{Z}_{(j,0)}^{(\kappa)} \otimes \mathbb{Z}_{(j,1)}^{(\kappa)} \right) \right) \otimes \bigotimes_{\xi=1}^{j-1} \left(\mathbb{Z}_{(j,0)}^{(\eta)} \otimes \mathbb{Z}_{(j,1)}^{(\eta)} \right) \otimes \mathbb{Z}_{(j,0)}^{(\eta)} \otimes \left(a^{+} \right)_{(j,1)}^{(\eta)} \ , \tag{3.34}$$

$$\Rightarrow \psi_{j,0}^{\dagger}\left(\eta a\right)$$
$$\rightarrow \frac{-1}{\sqrt{a}} \bigotimes_{\kappa=1}^{\eta-1} \left(\bigotimes_{\xi=1}^{N} \left(\mathbb{Z}_{(j,0)}^{(\kappa)} \otimes \mathbb{Z}_{(j,1)}^{(\kappa)} \right) \right) \otimes \bigotimes_{\xi=1}^{j-1} \left(\mathbb{Z}_{(j,0)}^{(\eta)} \otimes \mathbb{Z}_{(j,1)}^{(\eta)} \right) \otimes \left(a^{-} \right)_{(j,0)}^{(\eta)} \otimes \mathbb{I}_{(j,1)}^{(\eta)} \ , \tag{3.35}$$

$$\Rightarrow \psi_{j,1}^{\dagger}\left(\eta a\right)$$
$$\rightarrow \frac{-1}{\sqrt{a}} \bigotimes_{\kappa=1}^{\eta-1} \left(\bigotimes_{\xi=1}^{N} \left(\mathbb{Z}_{(j,0)}^{(\kappa)} \otimes \mathbb{Z}_{(j,1)}^{(\kappa)} \right) \right) \otimes \bigotimes_{\xi=1}^{j-1} \left(\mathbb{Z}_{(j,0)}^{(\eta)} \otimes \mathbb{Z}_{(j,1)}^{(\eta)} \right) \otimes \mathbb{Z}_{(j,0)}^{(\eta)} \otimes \left(a^{-} \right)_{(j,1)}^{(\eta)} \ , \tag{3.36}$$

$$\Rightarrow \bar{\psi}_{j,0}\left(\eta a\right)$$
$$\rightarrow \frac{-i}{\sqrt{a}} \bigotimes_{\kappa=1}^{\eta-1} \left(\bigotimes_{\xi=1}^{N} \left(\mathbb{Z}_{(j,0)}^{(\kappa)} \otimes \mathbb{Z}_{(j,1)}^{(\kappa)} \right) \right) \otimes \bigotimes_{\xi=1}^{j-1} \left(\mathbb{Z}_{(j,0)}^{(\eta)} \otimes \mathbb{Z}_{(j,1)}^{(\eta)} \right) \otimes \mathbb{Z}_{(j,0)}^{(\eta)} \otimes \left(a^{-} \right)_{(j,1)}^{(\eta)} \ , \tag{3.37}$$

$$\Rightarrow \bar{\psi}_{j,1}\left(\eta a\right)$$
$$\rightarrow \frac{i}{\sqrt{a}} \bigotimes_{\kappa=1}^{\eta-1} \left(\bigotimes_{\xi=1}^{N} \left(\mathbb{Z}_{(j,0)}^{(\kappa)} \otimes \mathbb{Z}_{(j,1)}^{(\kappa)} \right) \right) \otimes \bigotimes_{\xi=1}^{j-1} \left(\mathbb{Z}_{(j,0)}^{(\eta)} \otimes \mathbb{Z}_{(j,1)}^{(\eta)} \right) \otimes \left(a^{-} \right)_{(j,0)}^{(\eta)} \otimes \mathbb{I}_{(j,1)}^{(\eta)} \ , \tag{3.38}$$

where $a+ = \begin{pmatrix} 0 & 0 \\ 1 & 0 \end{pmatrix}$ and $a^- = \begin{pmatrix} 0 & 1 \\ 0 & 0 \end{pmatrix}$. As one can easily verify, the long tails of $\mathbb{Z}$ tensor products cancel out and we are left with local Hamiltonian terms. The Hamiltonian terms are explicitly mapped to:

$$H_0$$

$$\to \sum_{j=1}^{N} \sum_{\eta a \in \Omega} \left[\frac{i}{2a} \left(\left(a^-\right)_{(j,1)}^{(\eta)} \otimes \mathbb{Z}^{\otimes 2N-1} \otimes \left(a^+\right)_{(j,1)}^{(\eta+1)} - \left(a^-\right)_{(j,0)}^{(\eta)} \otimes \mathbb{Z}^{\otimes 2N-1} \otimes \left(a^+\right)_{(j,0)}^{(\eta+1)} \right) \right.$$

$$\left. - im_0 \left(a^+\right)_{(j,0)}^{(\eta)} \otimes \left(a^+\right)_{(j,1)}^{(\eta)} + h.c. \right] , \tag{3.39}$$

$$H_g$$

$$\to \frac{g_0^2}{2a} \sum_{\eta a \in \Omega} \left[\sum_{j=1}^{N} \left(\left(a^-\right)_{(j,0)}^{(\eta)} \otimes \left(a^+\right)_{(j,1)}^{(\eta)} - \left(a^+\right)_{(j,0)}^{(\eta)} \otimes \left(a^-\right)_{(j,1)}^{(\eta)} \right) \right]^2 , \tag{3.40}$$

$$H_w$$

$$\to \sum_{\eta a \in \Omega} \frac{r}{2a} \sum_{j=1}^{N} \left[i \left(a^-\right)_{(j,1)}^{(\eta)} \otimes \mathbb{Z}^{\otimes 2N-2} \otimes \left(a^+\right)_{(j,0)}^{(\eta+1)} + i \left(a^+\right)_{(j,0)}^{(\eta)} \otimes \mathbb{Z}^{\otimes 2N} \otimes \left(a^i\right)_{(j,1)}^{(\eta+1)} \right.$$

$$\left. - 2i \left(a^+\right)_{(j,0)}^{(\eta)} \otimes \left(a^-\right)_{(j,1)}^{(\eta)} + h.c. \right] . \tag{3.41}$$

And as we were expecting, all of these Hamiltonian terms are indeed local.

3.8 Bounds On The Error Incurred From Few-level Approximation

Here we present the proof of Theorem 2:

Proof. Starting with the same Hamiltonian as Eq. (3.24) we have:

$$H = H_0 + \lambda \cos(\omega t) W \ , \tag{3.42}$$

$$H_0|\psi_j\rangle = E_j|\psi_j\rangle \ . \tag{3.43}$$

Let's define ω_{ij} as:

$$\omega_{ij} = E_i - E_j \ . \tag{3.44}$$

Now, let's go to the interaction picture. That is, for any operator O let $O_I = e^{iH_0t}Oe^{-iH_0t}$. In particular, we will solve for the dynamics of

$$\rho_I = e^{iH_0t}\rho e^{-iH_0t}. \tag{3.45}$$

The interaction picture is convenient for treating the time-dependent perturbation terms in the Hamiltonian. For the evolution equation we have:

$$i\frac{d}{dt}\rho_I = \lambda \cos(\omega t) [W_I, \rho_I] \ , \tag{3.46}$$

where:

$$W_I(t) = e^{iH_0t}We^{-iH_0t} \ . \tag{3.47}$$

Note that our states are pure and we can switch between density matrix and state representation for convenience. Now let's decompose the Hilbert space into $\mathcal{H} = \mathcal{H}^{(+)} \oplus \mathcal{H}^{(-)}$ where:

$$\mathcal{H}^{(-)} = \text{span}\{|\psi_0\rangle, |\psi_1\rangle, \cdots, |\psi_{\nu-1}\rangle\} \ , \tag{3.48}$$

$$\mathcal{H}^{(+)} = \text{span}\left\{|\psi_\nu\rangle, |\psi_{\nu+1}\rangle, \cdots\right\} \ . \tag{3.49}$$

We are going to consider the more general few-level approximation; the few-level approximation is more applicable than the 2-level approximation when one's dealing with a system which has degeneracies. In this section we are trying to bound the error that incurs by limiting our Hilbert space to $\mathcal{H}^{(-)}$.

Let $P^{(A)}$ be the projector onto $\mathcal{H}^{(A)}$ for $A \in \{+, -\}$ and

$$W_I^{(AB)} = P^{(A)} W_I P^{(B)} \ . \tag{3.50}$$

The initial state is the ground state of the theory:

$$\rho_I(0) = |\psi_0\rangle\langle\psi_0| \ . \tag{3.51}$$

The few-level approximation is defined as:

$$\rho_I(t) \simeq \rho_I^{(-)}(t) \ , \tag{3.52}$$

where $\rho_I^{(-)}(t)$ is defined by:

$$\rho_I^{(-)}(0) = \rho_I(0) = |\psi_0\rangle\langle\psi_0| \ , \tag{3.53}$$

$$i\frac{d}{dt}\rho_I^{(-)} = \lambda\cos(\omega t)\left[W_I^{(--)}, \rho_I^{(-)}\right] . \tag{3.54}$$

Note that $\rho_I^{(-)} \neq P^{(-)}\rho_I P^{(-)}$. For simplicity, let's restrict our attention to the case

that W has no diagonal terms, *i.e.*

$$\langle \psi_j \left| W \right| \psi_j \rangle = 0 \ , \forall j \in \mathbb{N} \ . \tag{3.55}$$

Furthermore we assume the system is on resonance, $\omega_{10} = \omega$. We use the trace, $\mathbf{Tr}\left[\rho_I^{(-)}(t)\,\rho_I(t)\right]$, to quantify the error. We have:

$$\begin{aligned}
& i\tfrac{d}{dt}\mathbf{Tr}\left[\rho_I^{(-)}(t)\,\rho_I(t)\right] \\
& = i\mathbf{Tr}\left[\tfrac{d}{dt}\left(\rho_I^{(-)}(t)\,\rho_I(t)\right)\right] \\
& = \mathbf{Tr}\left[\lambda\cos(\omega t)\left[W_I^{(--)},\rho_I^{(-)}\right]\rho_I + \lambda\cos(\omega t)\,\rho_I^{(-)}\left[W_I,\rho_I\right]\right] \\
& = \lambda\cos(\omega t)\,\mathbf{Tr}\left[\left(W_I^{(--)} - W_I\right)\left[\rho_I^{(-)},\rho_I\right]\right] \\
& = \lambda\cos(\omega t)\,\mathbf{Tr}\left[W_I^{(-+)}(t)\,\rho_I(t)\,\rho_I^{(-)}(t) - W_I^{(+-)}(t)\,\rho_I^{(-)}(t)\,\rho_I(t)\right] \ .
\end{aligned} \tag{3.56}$$

The integral form of this equation becomes:

$$\begin{aligned}
& \mathbf{Tr}\left[\rho_I^{(-)}(t)\,\rho_I(t)\right] \\
& = 1 - i\lambda\int_0^t d\tau\cos(\omega t)\,\mathbf{Tr}\left[W_I^{(-+)}(t)\,\rho_I(t)\,\rho_I^{(-)}(t) - W_I^{(+-)}(t)\,\rho_I^{(-)}(t)\,\rho_I(t)\right] \ .
\end{aligned} \tag{3.57}$$

Now, if we expand the cosine function as the sum of two exponentials, we can write:

$$\left|\mathbf{Tr}\left[\rho_I^{(-)}(t)\,\rho_I(t)\right]\right| \geq 1 - K_1 - K_2 - L_1 - L_2 \ , \tag{3.58}$$

where

$$K_k = \frac{\lambda}{2}\left|\int_0^t d\tau e^{(-1)^k i\omega\tau}\mathbf{Tr}\left[W_I^{(-+)}(t)\,\rho_I(t)\,\rho_I^{(-)}(t)\right]\right| \ , \tag{3.59}$$

$$L_k = \frac{\lambda}{2}\left|\int_0^t d\tau e^{(-1)^k i\omega\tau}\mathbf{Tr}\left[W_I^{(+-)}(t)\,\rho_I^{(-)}(t)\,\rho_I(t)\right]\right| . \tag{3.60}$$

Using Eq. (3.47) we can rewrite K_k as:

$$\begin{aligned}
&K_k \\
&= \tfrac{\lambda}{2}\left|\int_0^t d\tau e^{(-1)^k i\omega\tau}\textstyle\sum_{\mu,\eta}\left\langle\psi_I^{(-)}(\tau)\left|{}_\mu W_I^{(-+)}(\tau)_{\mu\eta}\right|\psi_I(\tau)\right\rangle_\eta\left\langle\psi_I(\tau)\left|\psi_I^{(-)}(\tau)\right\rangle\right| \\
&= \tfrac{\lambda}{2}\left|\int_0^t d\tau e^{(-1)^k i\omega\tau}\textstyle\sum_{\mu=0}^{\nu-1}\sum_{\eta\geq m}\left\langle\psi_I^{(-)}(\tau)\left|{}_\mu\hat{W}_{\mu\eta}e^{i\omega_{\mu\eta}\tau}\right|\psi_I(\tau)\right\rangle_\eta\left\langle\psi_I(\tau)\left|\psi_I^{(-)}(\tau)\right\rangle\right| \\
&= \tfrac{\lambda}{2}\left|\textstyle\sum_{\mu=0}^{\nu-1}\sum_{\eta\geq\nu}\int_0^t d\tau e^{(-1)^k i\omega\tau+i\omega_{\mu\eta}\tau}\left\langle\psi_I^{(-)}(\tau)\left|{}_\mu\hat{W}_{\mu\eta}\right|\psi_I(\tau)\right\rangle_\eta\left\langle\psi_I(\tau)\left|\psi_I^{(-)}(\tau)\right\rangle\right| .
\end{aligned} \tag{3.61}$$

We calculate this integral using integration by parts:

$$\begin{aligned}
I_{k\mu\eta} &\equiv \textstyle\int_0^t d\tau e^{(-1)^k i\omega\tau+i\omega_{\mu\eta}\tau}\left\langle\psi_I^{(-)}(\tau)\left|{}_\mu\hat{W}_{\mu\eta}\right|\psi_I(\tau)\right\rangle_\eta\left\langle\psi_I(\tau)\left|\psi_I^{(-)}(\tau)\right\rangle\right. , \\
du_{k\mu\eta} &\equiv d\tau e^{(-1)^k i\omega\tau+i\omega_{\mu\eta}\tau} , \\
v_{\mu\eta} &\equiv \left\langle\psi_I^{(-)}(\tau)\left|{}_\mu\hat{W}_{\mu\eta}\right|\psi_I(\tau)\right\rangle_\eta\left\langle\psi_I(\tau)\left|\psi_I^{(-)}(\tau)\right\rangle\right. .
\end{aligned} \tag{3.62}$$

$$\Rightarrow\begin{cases}
u_{k\mu\eta} &= \frac{e^{\left[(-1)^k\omega+\omega_{\mu\eta}\right]i\tau}}{i\left[(-1)^k\omega+\omega_{\mu\eta}\right]} \\
dv_{\mu\eta} &= d\tau\frac{\lambda\cos(\omega\tau)}{i}\mathbf{Tr}\left[-W_I^{(+-)}\rho_I^{(-)}\hat{W}_{\mu\eta}\rho_I\right. \\
&\quad\left.+\left(\hat{W}_{\mu\eta}\left(W_I^{(++)}+W_I^{(+-)}\right)-W_I^{(--)}\hat{W}_{\mu\eta}\right)\rho_I\rho_I^{(-)}\right]
\end{cases} . \tag{3.63}$$

So $I_{k\mu\eta}$ becomes:

$$\begin{aligned}
I_{k\mu\eta} &= \tfrac{1}{i}\mathbf{Tr}\left[\rho_I^{(-)}(t)\,\hat{R}_{k\mu\eta}\rho_I(t)\right]\Big|_{\tau=0}^t \\
&\quad+\textstyle\int_0^t d\tau\lambda\cos(\omega\tau)\,\mathbf{Tr}\left[-W_I^{(+-)}\rho_I^{(-)}\hat{R}_{k\mu\eta}\rho_I\right. \\
&\quad\left.+\left(\hat{R}_{k\mu\eta}\left(W_I^{(++)}+W_I^{(+-)}\right)-W_I^{(--)}\hat{R}_{k\mu\eta}\right)\rho_I\rho_I^{(-)}\right] ,
\end{aligned} \tag{3.64}$$

where $\hat{R}_{k\mu\eta}(\tau)$ is defined as:

$$\hat{R}_{k\mu\eta}(\tau) = \frac{e^{\left[(-1)^k\omega+\omega_{\mu\eta}\right]i\tau}}{\left[(-1)^k\omega+\omega_{\mu\eta}\right]} W_{\mu\eta}\left|\psi_\mu\right\rangle\left\langle\psi_\eta\right| \ . \tag{3.65}$$

Now putting this back into Eq. (3.61) we get:

$$\begin{aligned} K_k = & \tfrac{\lambda}{2}\Big|\tfrac{1}{i}\Big\langle\psi_I^{(-)}(t)|R_k(t)|\psi_I(t)\Big\rangle\Big\langle\psi_I(t)|\psi_I^{(-)}\Big\rangle - \tfrac{1}{i}\langle\psi_I(0)|R_k(0)|\psi_I(0)\rangle \\ & + \int_0^t d\tau\lambda\cos(\omega\tau)\Big(\Big\langle\psi_I\Big|-W_I^{(+-)}\rho_I^{(-)}R_k+\rho_I^{(-)}\Big(R_k\Big(W_I^{(++)}+W_I^{(+-)}\Big)-W_I^{(--)}R_k\Big)\Big|\psi_I\Big\rangle\Big)\Big| \ , \end{aligned} \tag{3.66}$$

where from Eq. (3.65):

$$R_k = \sum_{\mu=0}^{\nu-1}\sum_{\eta\geq\nu}\frac{e^{\left[(-1)^k\omega+\omega_{\mu\eta}\right]i\tau}}{\left[(-1)^k\omega+\omega_{\mu\eta}\right]} W_{\mu\eta}\left|\psi_\mu\right\rangle\left\langle\psi_\eta\right| . \tag{3.67}$$

Hence, by the triangle inequality and submultiplicativity of the operator norm:

$$\begin{aligned} K_k \ & \leq \tfrac{\lambda}{2}\left(\|R_k(t)\|+\|R_k(0)\|\right) \\ & \quad + \tfrac{\lambda^2 t}{2}\max_{0\leq\tau\leq t}\Big(\Big(\Big\|W_I^{(++)}(\tau)+W_I^{(+-)}(\tau)\Big\| \\ & \quad + \Big\|W_I^{(-+)}(\tau)\Big\|+\Big\|W_I^{(--)}(\tau)\Big\|\Big)\|R_k(\tau)\|\Big) \\ & \leq \tfrac{\lambda}{2}\left(\|R_k(t)\|+\|R_k(0)\|+3\lambda t\max_{0\leq\tau\leq t}\left(\|W_I(\tau)\|\,\|R_k(\tau)\|\right)\right) \\ & \leq \tfrac{\lambda}{2}\left(\|R_k(t)\|+\|R_k(0)\|+3\lambda t\,\|W\|\max_{0\leq\tau\leq t}\left(\|R_k(\tau)\|\right)\right) \ . \end{aligned} \tag{3.68}$$

Note that $\|W_I(\tau)\| = \|W\| = 1$ for all τ. We can decompose $R_k(\tau)$ as the sum over the first index as:

$$R_k(\tau) = \sum_{\mu=0}^{\nu-1} R_k^\mu(\tau) \ , \tag{3.69}$$

where

$$R_k^\mu(\tau) = \sum_{\eta \geq \nu} \frac{e^{\left[(-1)^k \omega + \omega_{\mu\eta}\right] i\tau}}{\left[(-1)^k \omega + \omega_{\mu\eta}\right]} W_{\mu\eta} \left|\psi_\mu\right\rangle \left\langle\psi_\eta\right| \qquad \mu = 0, 1, \cdots, \nu - 1 \ . \tag{3.70}$$

So

$$\left\|R_k(\tau)\right\| \leq \left\|R_k^0(\tau)\right\| + \left\|R_k^1(\tau)\right\| + \cdots + \left\|R_k^{\nu-1}(\tau)\right\| \tag{3.71}$$

and

$$R_k^\mu(\tau) = P_\mu W D_k^\mu U_k^\mu(\tau) \ , \tag{3.72}$$

where

$$\begin{aligned} P_\mu &= \left|\psi_\mu\right\rangle \left\langle\psi_\mu\right| \qquad \mu = 0, 1, \cdots, \nu - 1 \ , \\ D_k^\mu &= \textstyle\sum_{\eta \geq \nu} \frac{\left|\psi_\eta\right\rangle \left\langle\psi_\eta\right|}{\left[(-1)^k \omega + \omega_{\mu\eta}\right]} \ , \\ U_k^\mu(\tau) &= \textstyle\sum_{\eta=0}^{\infty} e^{\left[(-1)^k \omega + \omega_{\mu\eta}\right] i\tau} \left|\psi_\eta\right\rangle \left\langle\psi_\eta\right| \ . \end{aligned} \tag{3.73}$$

One sees that $U_k^\mu(\tau)$ is unitary. So

$$\left\|R_k^\mu(\tau)\right\| \leq \left\|P_\mu\right\| \cdot \left\|W\right\| \cdot \left\|D_k^\mu\right\| . \tag{3.74}$$

P_μ is a projector so $\left\|P_\mu\right\| = 1$. $\left\|D_k^\mu\right\|$ is diagonal so it's easy to read its spectral norm:

$$\left\|D_k^\mu\right\| = \frac{1}{\delta_k^\mu} \ , \tag{3.75}$$

where

$$\delta_k^\mu = \min_{\eta > \nu} \left|(-1)^k \omega + \omega_{\mu\eta}\right| \ . \tag{3.76}$$

Thus Eq. (3.74) yields

$$\left\| R_k^{\mu}\left(\tau\right)\right\| \leq \frac{1}{\delta_k^{\mu}} \ . \tag{3.77}$$

Stitching Eqs. (3.77), (3.71) and (3.68)) together one gets:

$$K_k \leq \frac{\lambda}{2}\sum_{\mu=0}^{\nu-1}\left(\frac{2}{\delta_k^{\mu}}+3\lambda t\frac{1}{\delta_k^{\mu}}\right) \ . \tag{3.78}$$

Following the same procedure for L_k, one gets the same bound:

$$L_k \leq \frac{\lambda}{2}\sum_{\mu=0}^{\nu-1}\left(\frac{2}{\delta_k^{\mu}}+3\lambda t\frac{1}{\delta_k^{\mu}}\right) \ . \tag{3.79}$$

Hence Eq. (3.58) yields

$$\left|\mathbf{Tr}\left[\rho_I^{(-)}\left(t\right)\rho_I\left(t\right)\right]\right| \geq 1-\left(\lambda+\frac{3\lambda^2 t}{2}\right)\sum_{\mu=0}^{\nu-1}\sum_{k=1}^{2}\frac{1}{\delta_k^{\mu}} \ . \tag{3.80}$$

One sees that

$$\sum_{\mu=0}^{\nu-1}\sum_{k=1}^{2}\frac{1}{\delta_k^{\mu}} \leq \frac{2\nu}{\delta} \ , \tag{3.81}$$

where

$$\delta = \min\left\{\delta_k^{\mu} | \mu \in \{0,1,\cdots,\nu-1\}\ ,\ k\in\{1,2\}\right\} \ . \tag{3.82}$$

In other words, δ is the detuning to the nearest off-resonant transition from the first ν states. So the error caused by the ν-level approximation can be bounded:

$$\left|\mathbf{Tr}\left[\rho_I^{(-)}\left(t\right)\rho_I\left(t\right)\right]\right| = \left|\mathbf{Tr}\left[\rho^{(-)}\left(t\right)\rho\left(t\right)\right]\right| \geq 1-\left(2\nu\lambda+3\nu\lambda^2 t\right)\frac{1}{\delta} \ . \tag{3.83}$$

□

3.9 Bounds On The Error Incurred From Rabi Oscillations

Here we present a proof for Theorem 3:

Proof. After a $\frac{\pi}{2}$ rotation around the y-axis, we'll get:

$$H_r = -\frac{\Delta}{2}\mathbb{X} - \lambda\cos(\omega t)\mathbb{Z}\ . \tag{3.84}$$

As it is explained in [Den+16], an approximate solution to this Hamiltonian, which is valid for both weak and strong coupling is given by:

$$|\psi\left(t\right)\rangle_r = \alpha_0 e^{-i\epsilon_0 t}|u_0\left(t\right)\rangle_r + \alpha_1 e^{-i\epsilon_1 t}|u_1\left(t\right)\rangle_r\ , \tag{3.85}$$

where:

$$\begin{cases} \epsilon_0 &= \frac{1}{2}\left(-\omega - \sqrt{\left[\omega - \Delta J_0\left(\frac{2\lambda}{\omega}\right)\right]^2 + \Delta^2 J_1^2\left(\frac{2\lambda}{\omega}\right)}\right) \\ \epsilon_1 &= \frac{1}{2}\left(-\omega + \sqrt{\left[\omega - \Delta J_0\left(\frac{2\lambda}{\omega}\right)\right]^2 + \Delta^2 J_1^2\left(\frac{2\lambda}{\omega}\right)}\right) \end{cases} \tag{3.86}$$

and

$$|u_j\left(t\right)\rangle_r = \sum_{n=-\infty}^{\infty} e^{in\omega t}|u_{j,n}\rangle_r \qquad \text{for } j = 0, 1\ , \tag{3.87}$$

where J_0 and J_1 are Bessel functions of the first kind and:

$$\begin{cases} |u_{0,n}\rangle_r &= \frac{1}{\sqrt{2}} \begin{pmatrix} \cos\left(\frac{\theta}{2}\right) J_{n+1}\left(\frac{\lambda}{\omega}\right) + \sin\left(\frac{\theta}{2}\right) J_n\left(\frac{\lambda}{\omega}\right) \\ -\cos\left(\frac{\theta}{2}\right) J_{n+1}\left(-\frac{\lambda}{\omega}\right) + \sin\left(\frac{\theta}{2}\right) J_n\left(-\frac{\lambda}{\omega}\right) \end{pmatrix} \\ |u_{1,n}\rangle_r &= \frac{1}{\sqrt{2}} \begin{pmatrix} -\sin\left(\frac{\theta}{2}\right) J_{n+1}\left(\frac{\lambda}{\omega}\right) + \cos\left(\frac{\theta}{2}\right) J_n\left(\frac{\lambda}{\omega}\right) \\ \sin\left(\frac{\theta}{2}\right) J_{n+1}\left(-\frac{\lambda}{\omega}\right) + \cos\left(\frac{\theta}{2}\right) J_n\left(-\frac{\lambda}{\omega}\right) \end{pmatrix} \end{cases}, \tag{3.88}$$

where:

$$\tan(\theta) = \frac{\Delta J_1\left(\frac{2\lambda}{\omega}\right)}{\omega - \Delta J_0\left(\frac{2\lambda}{\omega}\right)} . \tag{3.89}$$

For the rest of this section, we assume exact resonance conditions, *i.e.* $\Delta = \omega$:

$$\tan(\theta) = \frac{J_1\left(\frac{2\lambda}{\omega}\right)}{1 - J_0\left(\frac{2\lambda}{\omega}\right)} . \tag{3.90}$$

Because we start in the ground state of our non-rotated Hamiltonian, Eq. (3.29), we need to rotate our system again to get:

$$\begin{cases} |u_{0,n}\rangle &= \frac{1}{\sqrt{2}} \begin{pmatrix} 1 & 1 \\ -1 & 1 \end{pmatrix} |u_{0,n}\rangle_r \\ |u_{1,n}\rangle &= \frac{1}{\sqrt{2}} \begin{pmatrix} 1 & 1 \\ -1 & 1 \end{pmatrix} |u_{1,n}\rangle_r \end{cases} . \tag{3.91}$$

The time dependent state of the system is:

$$|\psi(t)\rangle = \beta_0 e^{-i\epsilon_0 t} \sum_{n=-\infty}^{\infty} e^{in\omega t}|u_{0,n}\rangle + \beta_1 e^{-i\epsilon_1 t} \sum_{n=-\infty}^{\infty} e^{in\omega t}|u_{1,n}\rangle \ . \tag{3.92}$$

After setting the initial condition to:

$$|\psi(0)\rangle = \begin{pmatrix} 1 \\ \\ 0 \end{pmatrix} \ , \tag{3.93}$$

and using the Bessel function identity:

$$\sum_{n=-\infty}^{\infty} J_n(x) = 1 \ , \tag{3.94}$$

we'll find the coefficients β_0 and β_1 to be:

$$\begin{cases} \beta_0 & = \sin\left(\frac{\theta}{2}\right) \\ \\ \beta_1 & = \cos\left(\frac{\theta}{2}\right) \end{cases} \tag{3.95}$$

After a bit of simplification one can write the state of the system explicitly as:

$$|\psi(t)\rangle$$
$$= \begin{pmatrix} \sum_{k=-\infty}^{\infty} e^{2ik\omega t}\left(\frac{\sin\theta}{2} J_{2k+1}\left(\frac{\lambda}{\omega}\right)\left(e^{-i\epsilon_0 t} - e^{-i\epsilon_1 t}\right) + J_{2k}\left(\frac{\lambda}{\omega}\right)\left(\sin^2\left(\frac{\theta}{2}\right) e^{-i\epsilon_0 t} + \cos^2\left(\frac{\theta}{2}\right) e^{-i\epsilon_1 t}\right)\right) \\ \\ \sum_{k=-\infty}^{\infty} e^{(2k-1)i\omega t}\left(\frac{\sin\theta}{2} J_{2k}\left(\frac{\lambda}{\omega}\right)\left(e^{-i\epsilon_1 t} - e^{-i\epsilon_0 t}\right) - J_{2k-1}\left(\frac{\lambda}{\omega}\right)\left(\sin^2\left(\frac{\theta}{2}\right) e^{-i\epsilon_0 t} + \cos^2\left(\frac{\theta}{2}\right) e^{-i\epsilon_1 t}\right)\right) \end{pmatrix} . \tag{3.96}$$

From the ordinary RWA, we expect the maximum transition to the excited state to

happen around $t \simeq \frac{\pi}{\lambda}$.

Using Jacobi-Anger expansion, one can prove:

$$\begin{cases} \sum_{n=-\infty}^{\infty} e^{(2n)i\phi} J_{2n}(x) & = \cos(x\sin(\phi)) \\ \sum_{n=-\infty}^{\infty} e^{(2n-1)i\phi} J_{2n-1}(x) & = i\sin(x\sin(\phi)) \end{cases} . \tag{3.97}$$

We can use these to take care of the summations in Eq. (3.96):

$$\begin{aligned} \left|\langle 1|\psi\left(\tfrac{\pi}{\lambda}\right)\rangle\right| &= \left|\tfrac{\sin\theta}{2} e^{-i\pi\omega/\lambda}\left(e^{-i\pi\epsilon_1/\lambda} - e^{-i\pi\epsilon_0/\lambda}\right)\cos\left(\tfrac{\lambda}{\omega}\sin\left(\tfrac{\pi\omega}{\lambda}\right)\right)\right. \\ &\quad \left. -i\left(\sin^2\left(\tfrac{\theta}{2}\right)e^{-i\pi\epsilon_0/\lambda} + \cos^2\left(\tfrac{\theta}{2}\right)e^{-i\pi\epsilon_1/\lambda}\right)\sin\left(\tfrac{\lambda}{\omega}\sin\left(\tfrac{\pi\omega}{\lambda}\right)\right)\right| . \end{aligned} \tag{3.98}$$

In order to be able to express the last equation as a series in powers of $\left(\frac{\lambda}{\omega}\right)$, let's define $\kappa \equiv \sin\left(\frac{\pi\omega}{\lambda}\right)$. κ is highly sensitive to the ratio $\frac{\omega}{\lambda}$, but its value is bounded between:

$$-1 \leq \kappa \leq 1 \tag{3.99}$$

Up to the first nonzero order we get:

$$\left|\left\langle 1 \middle| \psi\left(\frac{\pi}{\lambda}\right)\right\rangle\right| \sim \left|1 - \left(\frac{1+\kappa^2}{2} + i\kappa e^{i\pi\omega/\lambda}\right)\left(\frac{\lambda}{\omega}\right)^2 + O\left(\left(\frac{\lambda}{\omega}\right)^4\right)\right| , \tag{3.100}$$

$$\Rightarrow 1 - \left|\left\langle 1 \middle| \psi\left(\frac{\pi}{\lambda}\right)\right\rangle\right| \sim \left|\left(\frac{\cos^2\left(\frac{\pi\omega}{\lambda}\right)}{2} + i\sin\left(\frac{\pi\omega}{\lambda}\right)\cos\left(\frac{\pi\omega}{\lambda}\right)\right)\right|\left(\frac{\lambda}{\omega}\right)^2 + O\left(\left(\frac{\lambda}{\omega}\right)^4\right) . \tag{3.101}$$

Maximizing the r.h.s. expression over its valid range of arguments and ignoring the

higher order terms, one finds:

$$1 - \left|\left\langle 1 \left| \psi\left(\frac{\pi}{\lambda}\right)\right\rangle\right| \leq \frac{1}{\sqrt{3}}\left(\frac{\lambda}{\omega}\right)^2 . \tag{3.102}$$

This is good enough for our purposes, but if one can do the experiment with high precision and high control over ω and λ; by choosing $\omega = \left(n + \frac{1}{2}\right)\lambda$, this can in principle be improved to:

$$\frac{\pi}{48}\left(\frac{\lambda}{\omega}\right)^4 + O\left(\left(\frac{\lambda}{\omega}\right)^5\right) \leq 1 - \left|\left\langle 1|\psi\left(\frac{\pi}{\lambda}\right)\right\rangle\right| \leq \frac{1}{\sqrt{3}}\left(\frac{\lambda}{\omega}\right)^2 + O\left(\left(\frac{\lambda}{\omega}\right)^4\right) . \tag{3.103}$$

□

3.10 Conclusion

By introducing our state preparation algorithm, we have significantly improved the performance of quantum algorithms for simulation of Fermionic QFT. Furthermore, unlike adiabatic state preparation, MPS-based state preparation should be applicable to the phases of the theory which are unconnected to the free theory. In particular, starting from the free theory, as one increases the coupling constant while keeping the bare mass fixed, the Gross-Neveu model exhibits a quantum phase transition at which the eigenvalue gap (*i.e.* physical mass) vanishes. On the other side of this transition the $\psi \to -\psi$ symmetry is spontaneously broken. Because of the vanishing gap (at least in the infinite volume limit) adiabatic state preparation may have problems producing the vacuum of the symmetry-broken phase. However,

an MPS-based method should be able to access this phase directly without having to cross a phase transition.

Although we only used Gross-Neveu to illustrate our new state preparation method, it should be applicable to other Fermionic models in one spatial dimension. Extending the techniques to two spatial dimensions, such as through the uses of Projected Entangled Pair States (PEPS) [STV11; Sch+13] is an interesting avenue for future research.

Chapter 4: Site-by-site quantum state preparation algorithm for preparing vacua of fermionic lattice field theories

4.1 Abstract

Answering whether quantum computers can efficiently simulate quantum field theories has both theoretical and practical motivation. From the theoretical point of view, it answers the question of whether a hypothetical computer that utilizes quantum field theory would be more powerful than other quantum computers. From the practical point of view, when reliable quantum computers are eventually built, these algorithms can help us better understand the underlying physics that govern our world.

In the best known quantum algorithms for simulating quantum field theories, the time scaling is dominated by initial state preparation. In this paper, we exclusively focus on state preparation and present a heuristic algorithm that can prepare the vacuum of fermionic systems in more general cases and more efficiently than previous methods. With our method, state preparation is no longer the bottleneck, as its runtime has the same asymptotic scaling with the desired precision as the remainder of the simulation algorithm. We numerically demonstrate the effectiveness

of our proposed method for the 1+1 dimensional Gross-Neveu model.

4.2 Introduction

One of the main motivations for building quantum computers is to simulate quantum systems efficiently [Fey82], something that is believed to be computationally hard on classical computers [Fey85]. Some scattering problems in Quantum Field Theories (QFTs) are BQP-complete [Jor+18], and are thus among the most difficult problems that a quantum computer is able to solve. Thus, generic QFTs cannot be simulated in polynomial time on a classical computer unless, of course, quantum computers are actually no more powerful than classical computers (i.e., BQP=BPP in the language of computational complexity theory). Although Monte Carlo simulations (e.g., for the lattice quantum chromodynamics) can yield static measures like binding energy, doing real-time dynamics for quarks has proven to be difficult [Chr10].

There are two main approaches to quantum simulation of quantum systems [Pre18; DM16; CZ12]. One approach is to design a system with many quantum degrees of freedom whose dynamics resemble a certain quantum system we want to study. This is called *Analog Quantum Simulation*. Research in this area has been vibrant in the past decade and a half, and possible quantum systems to embed the simulations include but are not limited to ultra cold atoms [BDN12], ion traps [BR12] and Rydberg atoms [Gla+14]. In particular, there are a number of proposals for simulating lattice gauge theories using ultracold atoms in optical lat-

tices [GZC17; Kas+17; Ban+12; Ric+18; ZB15]. Although some of these proposals for analog quantum simulation are quite promising and have been implemented in labs [Ber+17; Zha+17], they have to be handcrafted for each specific problem, and error analysis poses a challenge. The other approach is to use a universal, general purpose *Digital Quantum Computer* to simulate quantum systems. Starting with the pioneering works of [Fey82; Deu85b; Llo96; AL97; Zal98], quantum algorithms for simulating quantum systems using universal digital quantum simulation have become a well-developed area of study.

The known digital quantum algorithms for calculating scattering amplitudes in QFT consist of at least four distinct subroutines [JLP12; JLP14; HJ18; KS19a; KS19b]. First, they prepare the vacuum state, either by directly preparing the ground state of the interacting theory [HJ18], or by first preparing the ground state of the noninteracting theory and then adiabatically turning on the interactions [JLP14]. The next step is to prepare incoming particle states by adding oscillating terms to the Hamiltonian that couple the vacuum to the desired excited states. Reference [JLP12] actually does these two steps in a slightly different manner, by exciting the particles in the noninteracting theory and then adiabatically turning on the interactions. The third step is to let the particles interact and scatter. This is achieved by using an efficient Hamiltonian simulation algorithm, like the ones introduced in Refs. [LC16b; Haa+18; Ber+14]. The last step is to measure properties of the outgoing particles, such as their locations or momenta. This can be achieved by either adiabatically tuning back to the noninteracting theory or by measuring some local charges with phase estimation [JLP14].

The first two steps together can be thought as the initialization phase of algorithm. In the previous results, initialization has been the bottleneck of the QFT simulation algorithms. For this reason, here we only focus on improving this part of the algorithm, specifically preparation of the vacuum of the interacting theory. The performance of Refs. [JLP12; JLP14] is limited by slow adiabatic transitions in order to avoid exciting extra particles. Reference [HJ18] improves upon the fermionic result by using Matrix Product State properties of one dimensional systems and a classical heuristic algorithm known as the density-matrix renormalization group (DMRG); however, its applications are mostly limited to one dimensional systems and the performance is limited by the classical part of the algorithm [1]. In principle, quantum computational power could be used to circumvent this classical bottleneck.

In this paper, we present an efficient method for initial state preparation that is inherently quantum and generalizes to fermionic QFTs in any number of dimensions. We numerically demonstrate its performance in a 1+1 dimensional fermionic QFT, namely the Gross-Neveu model [GN74]. In this case in the asymptotic limit of infinite precision for constant system size, the expected performance of this state preparation method scales at least as well with the precision goal ϵ as the remaining steps in the simulation algorithm. We expect similar performance gains would hold more generally.

In spirit, our algorithm is related to Schwartz, Temme and Verstraete's al-

[1] It is important to note that results like [SPC11] that imply gapped one dimensional systems are in the same phase and therefore can be prepared in constant time, do not apply here. In particular they assume that the ratio between correlation length of the system and lattice spacing does not increase with adding more sites to the system. However, in these simulation algorithms one typically assumes system size to be fixed and lattice step decreasing with more sites.

gorithm for preparing injective *Projected Entangled Pair States* (PEPS) [STV11]. Their algorithm and ours both grow the system size by adding one site at a time. The main difference is that in their case one needs to know an injective PEPS representation for the state they are preparing, while our algorithm does not. Also, our algorithm performs better with regards to the precision goal ϵ.

The structure of this manuscript is as follows: In Sec. 4.3 we lay out two lemmas and a theorem which are the theoretical foundations of the paper. These are then utilized in Sec. 4.4, which is concerned with explaining our algorithm. Section 4.5 introduces the fermionic Gross-Neveu model as a testbed for our algorithm. Specifically, in Sec. 4.5.1 we review the model, and in Sec. 4.5.2 we provide numerical evidence that our algorithm applies to it. Finally, we conclude in Sec. 4.6.

4.3 Preliminaries

Aharonov and Ta-Shma in a seminal paper showed that if two states have non-negligible overlap, with some physically motivated assumptions, one can transition between them in time polynomial in system size [AT07]. The current paper was in part inspired by their Jagged Adiabatic Path Lemma; however, in the current paper we are using another approach that relies on more modern techniques.

Lemma 3 (Phase estimation with $O((n/m)\log(1/\epsilon))$ gates)**.** *Given a simulatable Hamiltonian, H, that acts on n qubits, and a state, $|\psi\rangle$, and a promised lower bound on the spectral gap, $\Delta(H) > m$, and an estimate for the ground energy, $\tilde{E}$, with a promise that $\left|\tilde{E} - E\right| < \frac{m}{2}$, where E is the actual ground energy; we*

can check whether $|\psi\rangle$ is the ground state of H or not in runtime proportional to $O((n/m)\log(1/\epsilon))$, where ϵ is the probability of making a faulty decision.

Proof. An $O(\frac{n}{m\epsilon})$ performance can be achieved using the standard phase estimation algorithm [NC00]. To achieve the $O(\frac{n}{m}\log(1/\epsilon))$ scaling, one can coherently write the output of phase estimation to a number of qubits and then use majority vote and Chernoff bounds to boost the precision [Che52; Che81; Nie11]. Specifically, the phase estimation algorithm yields the energy of the state, which we can compare to the given estimate to decide whether it is the ground state or not. In order to achieve linear scaling with n, we need to implement a modern and efficient simulation algorithm for local Hamiltonians such as the ones in Ref. [CS19] or Ref. [Haa+18]. □

Lemma 4 (Mapping overlapping ground states [YLC14])**.** *Given two simulatable Hamiltonians, H_1 and H_2, with known ground energies, E_1 and E_2, and a minimum overlap between their ground states, $|\langle g_1|g_2\rangle| \geq \eta$, one can get from one ground state to the other with $O\left(\frac{\log(2/\epsilon)}{\eta}\right)$ oracle calls to the phase estimation algorithm on these Hamiltonians, where ϵ is the precision goal of the algorithm.*

Proof. This lemma is a direct result of Yoder *et. al.*'s Grover-esque fixed point quantum search [YLC14], when one replaces the oracle in their paper with our phase estimation from Lemma 3. □

Theorem 4 (Modified Jagged Path Lemma)**.** *Let us assume $\{H_j\}_{j=1}^{N}$ is a sequence of explicit bounded-norm and geometrically local Hamiltonians in a fixed number of dimensions that act on at most n qubits with nonvanishing spectral gaps, $\Delta(H_j) \geq$*

$m_j \geq 0$, where m_j are real positive constants. This means that each Hamiltonian H_j in the sequence is simulatable. Let us also assume we have a priori estimates of the ground energies of these Hamiltonians within accuracy better than half their spectral gap. Then, if the overlap between consecutive ground states, $|g_j\rangle$ and $|g_{j+1}\rangle$, is nonvanishing, $|\langle g_j|g_{j+1}\rangle| \geq \eta > 0$, there exists an efficient quantum algorithm that can start from $|g_1\rangle$ and output $|g_N\rangle$ with asymptotic runtime of $O\left(\frac{Nn}{m\eta}\,\mathrm{polylog}(1/\epsilon)\right)$, where ϵ is the maximum trace distance of the final state compared to the desired eigenstate and $m = \min\{m_j\}_{j=1}^{N}$.

Proof. We prove this theorem constructively.

- We use Lemma 4 to transform each ground state in the sequence, $|g_j\rangle$ to $|g_{j+1}\rangle$. Each oracle call is given by the phase estimation from Lemma 3. Thus, each transformation takes at most $O\left(\frac{n}{m\eta}\,\mathrm{polylog}(1/\epsilon)\right)$ gates.

- Because there are N states in the sequence, the overall runtime will be of order $O\left(\frac{Nn}{m\eta}\,\mathrm{polylog}(1/\epsilon)\right)$.

□

4.4 Overview of the Algorithm

4.4.1 1+1 dimensions

There already exist efficient quantum algorithms for preparing the vacuum state of a 1+1 dimensional quantum field theory [HJ18]. Nevertheless, we here use a 1+1 dimensional quantum field theory as a test case for our algorithm, in order

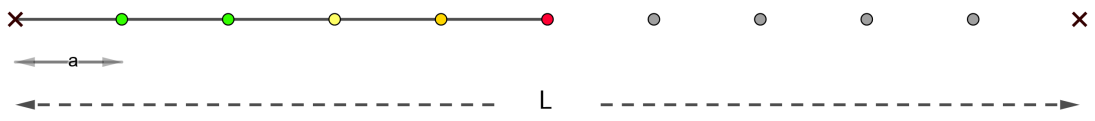

Figure 4.1: (color online) Adding an extra site to a 1D lattice. The crosses represent the boundary (Dirichlet). With a limited correlation length we expect only sites within that distance to be affected by adding an extra site to the system.

to numerically investigate the key unknown quantities determining its performance, namely the state overlaps η. For now we assume Dirichlet boundary conditions [CJO19], although it is easy to generalize the algorithm. The input of the algorithm is a continuous gapped one-dimensional Hamiltonian H, system length L, maximum error ϵ and an array of quantum registers initialized in the standard basis, Q. Each register consists of qubits which together represent the state of a single site. The output should be an approximation to the vacuum of H on the array Q that can yield cross sections with precision better than ϵ.

If the system size is much larger than the correlation length of the system, χ, then the inner products should reach a stable value, as the systems are basically unaffected by adding an extra site (Fig. 4.1). If the asymptotic value of this inner product is nonzero, it means that if the initial system is larger than a certain size, we can build the vacuum by inductively adding more sites.

4.4.2 Higher dimensions

In higher spatial dimensions, the algorithm is similar to 1+1 dimensions, with the difference that the discretization of the Hamiltonian is more involved and the order of adding extra sites is not uniquely defined.

Suppose the system volume is $V = L_1 \times L_2 \times \cdots \times L_D$. Then, in the high precision asymptotic limit, the lattice spacing should be $a \sim \epsilon$, where ϵ represents the maximum relative error of the scattering amplitudes. However, in the high energy limit, the wavelength of the particles would be the deciding factor and $a \sim p^{-1}$, where p represents the momentum of the incoming particles. Similar to the 1+1 dimensional case, one can take $a \sim \epsilon/p$ to respect both asymptotic limits simultaneously [JLP14].

As for the order of adding new sites, one reasonable method is to try to keep it as close to a D-dimensional hypercube as possible. Figure 4.2 can be seen as an example of how one can do this in two spatial dimensions, or the side of a three dimensional cube.

4.4.3 The algorithm

In general, our proposal for this state preparation algorithm is as follows. Let us assume our Hamiltonian lies in D spatial dimensions, and its volume is $V = L_1 \times L_2 \times \cdots \times L_D$. Also, let ϵ be the precision goal of the entire scattering simulation. Then do the following:

- Set the lattice spacing, a, as $a \propto \epsilon/p$.
- Properly discretize the Hamiltonian. This means replacing derivatives with finite differences and dealing with discretizing issues such as fermion doubling [Wil74; JLP14].
- Given a boundary condition (e.g. Dirichlet), prepare the ground state, $|g_{N_0}\rangle$, of

the discretized Hamiltonian with $N_0 \ll N = \frac{V}{a^D}$, i.e. a small constant number of sites.

- Apply a unitary gate (e.g. Hadamard) on the rest of the qubits, $|Q_j\rangle \forall j \in \{N_0 + 1, \ldots, N\}$, which is hoped to provide a reasonable overlap between states in the next phase of the algorithm (see Sec. 4.5.2.3).

As before, there is only one step in the iterative phase of the algorithm:

- For every $j \in \{N_0, \ldots, N-1\}$, transform $|g_j\rangle \otimes |Q_{j+1}\rangle$ to $|g_{j+1}\rangle$ by applying Theorem 4.

This yields a runtime of $O\left(\frac{V^2}{a^{2D}\eta} \operatorname{polylog}(1/\epsilon)\right)$. For the sake of clarity, we will include a conjecture that captures the unproven physical intuition that goes into this algorithm.

Conjecture 1 (Overlap of ground states)**.** *Assume a properly discretized massive fermionic QFT that obeys the Wightman axioms, in particular, the energy-momentum spectral condition [Str04]. Let $|g_j\rangle$ be the ground state of the system with j sites and η be defined as $\lim_{j\to\infty} |(\langle g_j| \otimes \langle Q|)\, |g_{j+1}\rangle|$, where $|Q\rangle$ is an unentangled state that is present to make the Hilbert spaces compatible. Then there exists $|Q\rangle$ for which $\eta > 0$.*

The value η is provably nonzero in many cases, for example if the ground states are described as injective PEPS [STV11] or if they are topological PEPS [Sch+13].

Some quantum systems will admittedly have ground states that seem to counter the conjecture above. For example, in the AKLT model [Aff+87], the overlap be-

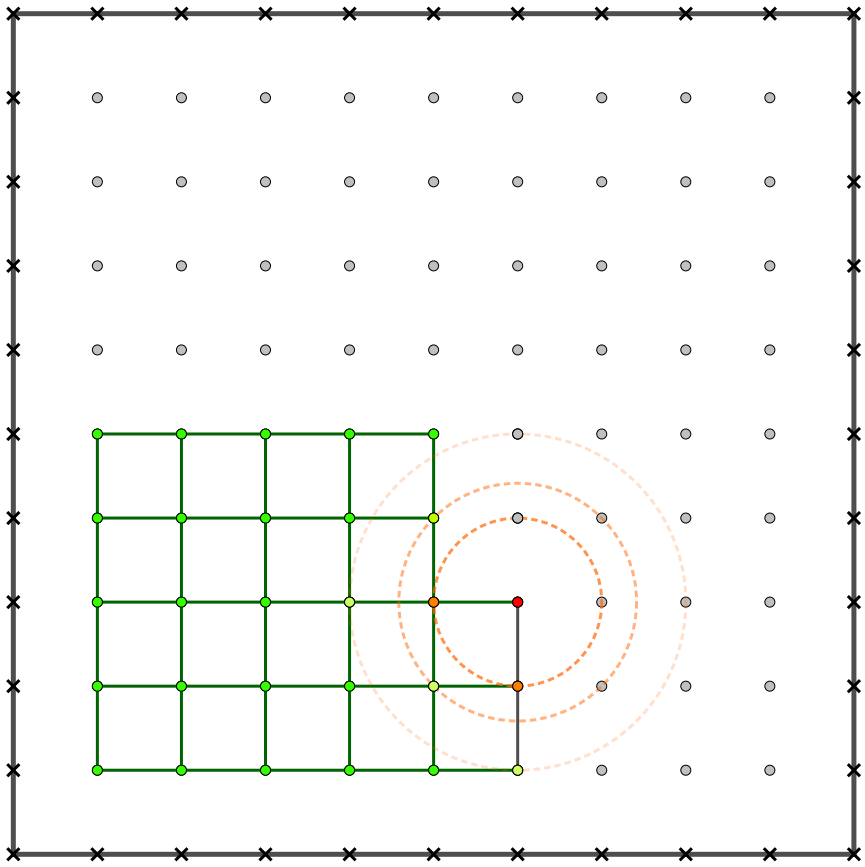

Figure 4.2: (color online) Adding an extra site to a 2D lattice. Because of limited correlation length, only few sites are expected to be affected by the introduction of a new site to the system.

tween consecutive ground states is provably zero. However, upon further investigation, one realizes that the AKLT model does not have a single site coarse continuum limit and you need to keep two sites at a time [De +18]. By adding two sites at a time, one can in fact get nonzero and constant overlap between the ground states.

4.5 Gross-Neveu model

4.5.1 Overview of the model

In this section we will introduce the Gross-Neveu model and use it as a test case for our proposal. The model was introduced in 1974 as a toy model for quantum chromodynamics [GN74]. It is a fermionic QFT that lives in 1+1 spacetime dimensions and exhibits different particle flavors as well as asymptotic freedom. It was originally defined as a massless theory, which has chiral symmetry. We explicitly break this symmetry by introducing a mass term in the Hamiltonian. The Lagrangian for the massive theory with $\mathcal{N}$ species is given by:

$$\mathcal{L} = \sum_{j=1}^{\mathcal{N}} \bar{\psi}_j \left(i\gamma^\mu \partial_\mu - m\right) \psi_j + \frac{g^2}{2} \left(\sum_{j=1}^{\mathcal{N}} \bar{\psi}_j \psi_j \right)^2 , \tag{4.1}$$

where g represents the interaction strength, γ^μ are two-dimensional representations of the Dirac field, $\bar{\psi} = \psi^\dagger \gamma^0$, and each field ψ_j has two components [JLP14]. We use the Majorana representation for the γ matrices, where they are explicitly written as:

$$\gamma^0 = i \begin{pmatrix} 0 & -1 \\ 1 & 0 \end{pmatrix} , \tag{4.2}$$

$$\gamma^1 = -i \begin{pmatrix} 0 & 1 \\ 1 & 0 \end{pmatrix} . \tag{4.3}$$

For simulation purposes it is more convenient to work with the equivalent

Hamiltonian formalism. Additionally, to simulate the scattering process on a digital quantum computer we need to discretize the model and put it on a lattice. Discretizing the model and putting it on a lattice introduces extra fermions; this is known as the fermion doubling problem [NN81b; NN81a]. These extra fermions can be handled via different methods such as Wilson fermions [Wil74], Kogut-Susskind staggered fermions [KS75; BSK76; Sus77] or domain wall fermions [Kap92]. For instance, if we had periodic boundary conditions and we had wanted to utilize Wilson fermions, we would have had to add an extra term to the Hamiltonian that decouples the extra fermions from the ground state (Fig. 4.3). The full Hamiltonian of the system after discretizing would then be [HJ18]:

$$H = H_0 + H_g + H_W \,, \tag{4.4}$$

where

$$H_0 = \sum_{x\in\Omega} a \sum_{j=1}^{\mathcal{N}} \sum_{\alpha,\beta\in\{0,1\}} \bar{\psi}_{j,\alpha}(x) \left[-i\gamma^1_{\alpha\beta} \frac{\psi_{j,\beta}(x+a) - \psi_{j,\beta}(x-a)}{2a} + m_0 \delta_{\alpha,\beta} \psi_{j,\beta}(x) \right] , \tag{4.5}$$

$$H_g = -\frac{g_0^2}{2} \sum_{x\in\Omega} a \left(\sum_{j=1}^{\mathcal{N}} \sum_{\alpha\in\{0,1\}} \bar{\psi}_{j,\alpha}(x) \psi_{j,\alpha}(x) \right)^2 , \tag{4.6}$$

$$H_W = \sum_{x\in\Omega} a \sum_{j=1}^{\mathcal{N}} \sum_{\alpha\in\{0,1\}} \left[-\frac{r}{2a} \bar{\psi}_{j,\alpha}(x) \left(\psi_{j,\alpha}(x+a) - 2\psi_{j,\alpha}(x) + \psi_{j,\alpha}(x-a) \right) \right] . \tag{4.7}$$

Here, H_0 represents the noninteracting term of the Hamiltonian, H_g represents the interaction term, and H_W is the Wilson term. The summation variable $j \in$

$\{1, 2, \ldots, \mathcal{N}\}$ indicates the fermion species, and $0 < r \leq 1$ is called the Wilson parameter. H is spatially local in the sense that it consists only of single-site and nearest-neighbor terms on the lattice.

If one wants to simulate the continuum limit of the Gross-Neveu model, they should eliminate the doubled fermions through some mathematical procedure. However, in our minimal approach for a numerical example, it suffices to note that the extra particles are not necessarily a problem. In our test example, the doubled fermions can be thought as extra flavors of fermions.

The $\mathcal{N} = 1$ case of the massive Gross-Neveu model, which we will be using to check our proposal, is equivalent to the massive Thirring model, which in turn can be solved analytically using Bethe ansatz [Hal82; Man75; Col75; Kor79; Okw83; ZZ79]. Although Bethe ansatz is a powerful tool, it does not work for all systems, and in this specific case the solutions are rather complicated. Instead, we focus here on more general numerical approaches, which can in principle work for arbitrary $\mathcal{N}$. Specifically, we rely on a DMRG algorithm [Sch11] to classically calculate the ground state as a Matrix Product State. The DMRG code we developed is written in Julia [Bez+17] and is available online [Ham19].

4.5.2 Numerical analysis and diagrams

Ideally, if one had access to a sufficiently advanced quantum computer, one might first choose the desired simulation parameters and then use them to determine the system size that is necessary for accurate simulation at that point. However,

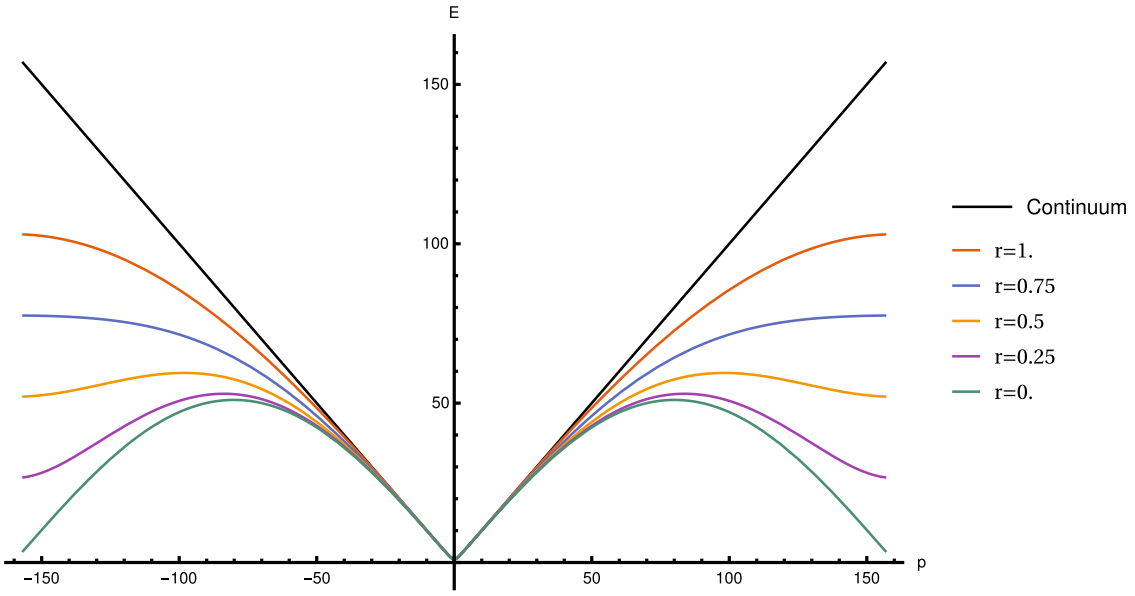

Figure 4.3: (color online) The dispersion relation of the non-interacting theory for different values of the Wilson parameter, r, compared to the continuum limit. In this plot m_0 is set to be $m_0 = 1$ and the descretized system is set to have unit length with $N = 50$ sites. The dispersion relation in this case is given by [JLP14]: $E^{(a)}_{m_0}(\mathbf{p}) = \sqrt{\left(m_0 + \frac{2r}{a}\sin^2\left(\frac{|\mathbf{p}|a}{2}\right)\right)^2 + \frac{1}{a^2}\sin^2\left(|\mathbf{p}|\,a\right)}\,.$

with limited classical computational power, we can only verify our proposal for reasonably small system sizes. Therefore, we aim to find a range of parameters, m_0, g_0, that can be simulated accurately on a system with ~ 50 sites. Specifically, the parameter regimes we choose must yield ground states with correlation lengths that are simultaneously much smaller than our simulation size and much larger than the lattice spacing.

4.5.2.1 Mass renormalization

If the interaction strength is set to zero (i.e., we are working in the free theory), then it is straightforward to calculate the two-point correlation functions in the continuum limit.

$$\psi(x) = \int \frac{dp}{2\pi} \frac{1}{\sqrt{2E_p}} \left(a(p)u(p)e^{-ip\cdot x} + b^\dagger(p)v(p)e^{ip\cdot x} \right) \ , \tag{4.8}$$

where $E_p = \sqrt{p^2 + m_0^2}$, $u(p) = \begin{pmatrix} \sqrt{E_p - p} \\ i\sqrt{E_p + p} \end{pmatrix}$, and $v(p) = \begin{pmatrix} \sqrt{E_p - p} \\ -i\sqrt{E_p + p} \end{pmatrix}$. $a(p)$ and $b^\dagger(p)$ are creation and annihilation operators. Then the two-point correlation function can be calculated as:

$$\begin{aligned} \langle 0|\psi_0(x)\bar{\psi}_0(y)|0\rangle &= \int \frac{dp\,dq}{(2\pi)^2} \frac{1}{2\sqrt{2E_pE_q}} e^{i(qy-px)} \\ &\quad \times \sqrt{E_p - p}\sqrt{E_q + q}\langle 0|a(p)a^\dagger(q)|0\rangle \qquad (4.9) \\ &= \int_{-\infty}^{\infty} \frac{dp}{2\pi} \frac{m_0}{2\sqrt{p^2 + m_0^2}} e^{ip(x-y)} \qquad (4.10) \\ &= \frac{m_0}{2\pi} K_0 \left(m_0 \left| x - y \right| \right) \ , \qquad (4.11) \end{aligned}$$

where K_0 is the modified Bessel function of the second kind. We expect the two-point correlation functions to keep such a form even in the discretized and interacting case, i.e.,

$$\langle 0|\psi_0(x)\bar{\psi}_0(x + \Delta x)|0\rangle \propto K_0 \left(\frac{\Delta x}{\chi(m)} \right) + O(\epsilon) \ , \tag{4.12}$$

where $\chi(m) \propto 1/m$ is the correlation length, which is generally inversely proportional to the renormalized mass. Asymptotically, $K_0(\zeta)$ behaves like an exponentially decaying function in the limit $\zeta \to \infty$ [HK06]:

$$K_0(\zeta) \sim \sqrt{\frac{\pi}{2\zeta}} e^{-\zeta} \left(1 - \frac{1}{8\zeta} + \frac{9}{128\zeta^2} + O\left(\frac{1}{\zeta^3} \right) \right) \ . \tag{4.13}$$

Going forward, we use an exponentially decaying form to numerically calculate the renormalized mass from the two-point correlation functions.

4.5.2.2 Bare mass and interaction strength

We investigate a range of values for bare mass, m_0, and interaction strength, g_0, specifically looking for the sets of parameters that yield correlation lengths that are much longer than our lattice spacing and at the same time much smaller than the system size. Because we have set the length of the system to be 1 (in units of inverse energy), a reasonable correlation length should be around $\sqrt{\frac{1}{51}} \approx \frac{1}{7.14}$, or about 7 lattice spacings. The goal of the rest of this subsection is not to pinpoint the parameters that nail such a correlation length, but rather find values that yield viable correlation lengths that ensure the calculations in the following subsections are valid.

After some preliminary calculations it seems that a good range of parameters that yield reasonable correlation lengths would be $g_0^2 \in [0, 2.0]$ and $m_0 \in [0.2, 0.4]$. We calculate the two-point correlation function, $\left\langle \psi_0\left(\frac{1}{2} - \frac{\Delta x}{2}\right) \bar{\psi}_0\left(\frac{1}{2} + \frac{\Delta x}{2}\right)\right\rangle, \forall x \in \{a, 2a, \ldots, \frac{N}{2}a\}$, of the system for a uniform distribution of parameters in that range. (Some of these two-point correlation functions can be seen in Fig. 4.4.) Equation (4.12) should hold for distances much larger than the lattice spacing. Therefore, ideally we are interested in the long range behavior of these correlation functions. However, at very long distances because of boundary effects and limited machine precision, our numerics deviate from Eq. (4.12). In order to avoid these issues, we

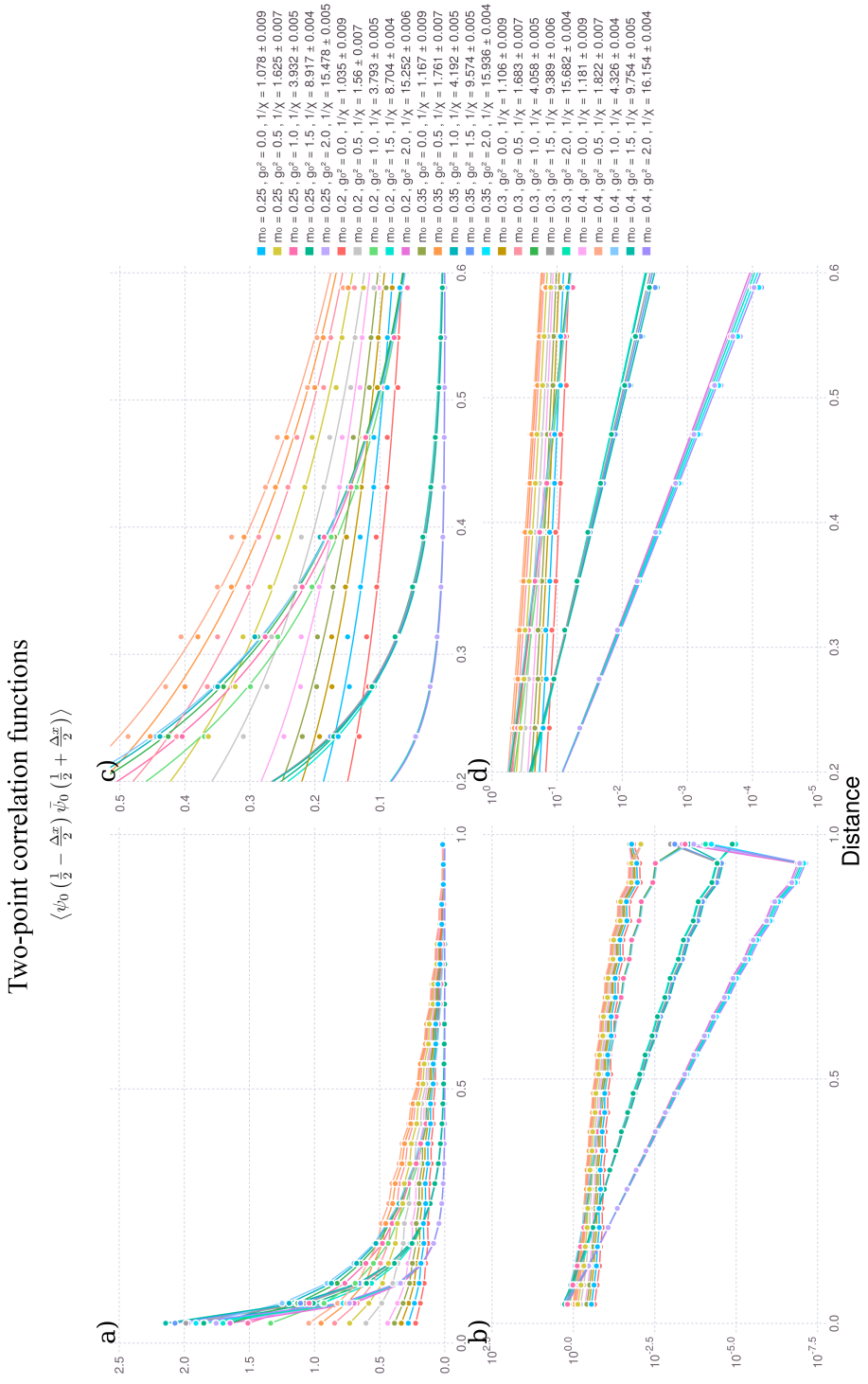

Figure 4.4: (color online) A sample of two-point correlation functions calculated for different set of m_0 and g_0^2 parameters. In subplots a) and b) we can see the entirety of the two correlation functions calculated over the span of distances. In subplots c) and d) we have only kept a range of distances in the middle. Also, the curves in these two subplots are the result of fitting $bK_0(\frac{\Delta x}{\chi})$ to the date points. The legend on the right shows parameters m_0 and g_0^2 for each set of data points as well as the inverse of the calculated correlation length, $\frac{1}{\chi}$.

hand pick a range of distances that are much larger than the lattice spacing and at the same time are far enough from the edge of the system. This range of distances shows the least amount of deviations. We determine the correlation length, χ, by finding the best set of values, b and χ, that fit the data with $bK_0\left(\frac{\Delta x}{\chi}\right)$.

Based on the results in Fig. 4.4, we deem parameters $(m_0 = 0.2, g_0^2 = 1.5)$ and $(m_0 = 0.4, g_0^2 = 1.0)$ to have correlation lengths suitable for further numerical calculations at the desired system size of $N = 50$.

4.5.2.3 Inner products

Now that we have found a set of reasonable parameters, let us look at the inner product between the ground states of systems with different numbers of lattice sites. In order to make the inner product well defined, we need to add unentangled extra sites to the smaller system so the Hilbert spaces will be the same. The extra site we add in our numerical analysis is a uniform superposition over the standard basis. In the case of $\mathcal{N} = 1$, we need two qubits per site after mapping the fermionic system to qubits using a Jordan-Wigner [JW28; BO00] transformation (see Ref. [HJ18] for a detailed explanation of this mapping for the Gross-Neveu model). The state of the extra site would be:

$$\frac{1}{2}\sum_{j=0}^{3}|\bar{j}\rangle\,, \tag{4.14}$$

where the bar in $\bar{j}$, means it is written in base 2 [2]. Now that the inner product is well defined, we increase the number of lattice sites, one at a time, and calculate the inner product between these ground states. As can be seen in Fig. 4.5, the inner products rapidly converge to a positive constant. This shows that our conjecture works for these sets of parameters of the Gross-Neveu model. Therefore, assuming we can classically estimate ground energies, our algorithm can be used to prepare their ground states.

With a back of the envelope calculation we expect the asymptotic value of the overlap, $\eta = \lim_{j\to\infty} \left(\langle g_j| \otimes \langle Q_{j+1}|\right) |g_{j+1}\rangle$, to be $\eta \propto e^{-\chi/a}$ in one spatial dimension. (In D spatial dimensions we expect this to be $\eta \propto \exp\left(-\frac{\chi^D}{a^D}\right)$, as more sites are affected by the introduction of a new site to the system.) However, what we observe in Fig. 4.5 shows inner products of surprisingly large magnitude and mild dependence on correlation length. We were surprised by this result, though it is good news for our algorithm, and we hope in the future to investigate additional lattice models to find out how generally it holds.

4.5.2.4 Predicting the energy

There is still one condition from Theorem 4 that needs to be satisfied before we can prepare the vacuum of the Gross-Neveu model using that theorem: We should

[2] Note that in most cases, especially systems that have conserved quantum numbers, this would not yield the maximum inner product. For example, in our case of the massive Gross-Neveu model, by choosing the extra site to be in the $(|01\rangle + |10\rangle)/\sqrt{2}$ state, one can improve the inner products by a factor of $\sqrt{2}$. Choosing the best state for the extra site requires some knowledge about the symmetries of the system, which in many cases can be difficult to know before doing deep analysis of the system. Therefore, to be conservative, we decided to use the more generic uniform superposition for the added site.

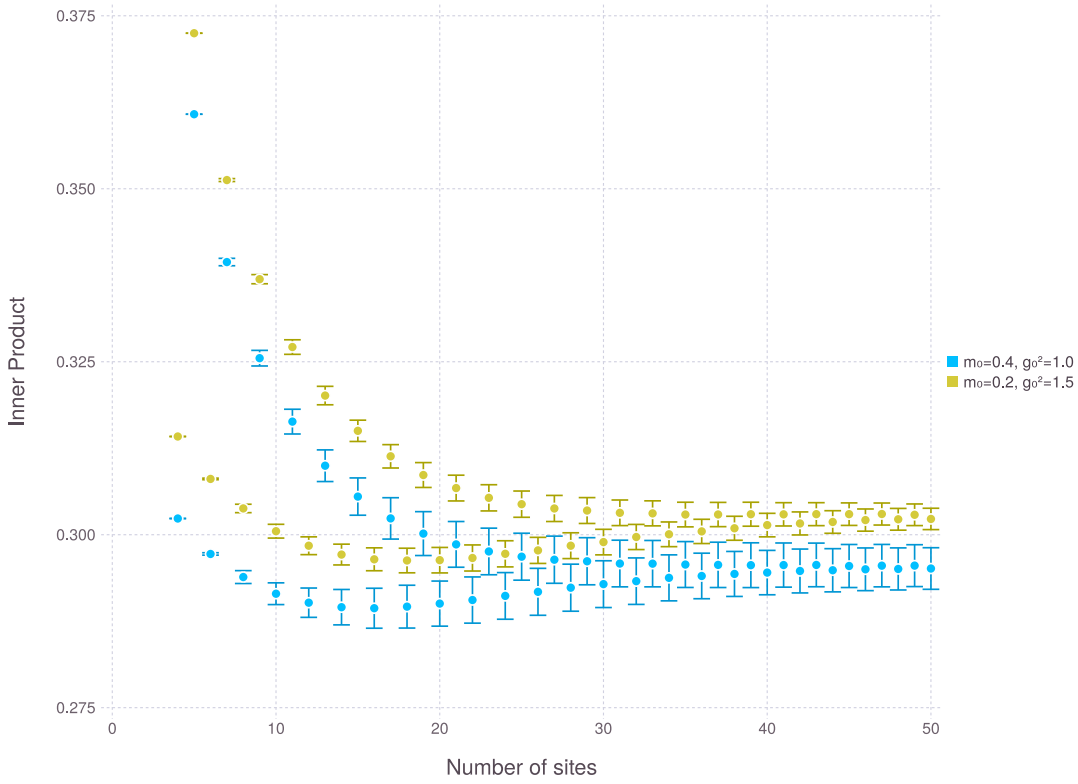

Figure 4.5: (color online) Inner products between systems with different numbers of lattice sites. The inner products are calculated for $(m_0 = 0.2, g_0^2 = 1.5)$ and $(m_0 = 0.4, g_0^2 = 1.0)$.

be able to predict the ground state energy with accuracy better than half of the gap. The gap is equal to the renormalized mass. The ground state energy is expected to grow almost linearly with the number of lattice sites with minute corrections from the Casimir effect. Therefore, the ground state energy can be approximated as [BMM01]:

$$E_g(L) = C_0 + C_1 L + C_2 \sum_{h=1}^{\infty} \frac{1}{h^2} K_2 \left(C_3 h L\right) \tag{4.15}$$

$$\approx c_0 + c_1 L + \frac{c_2}{L} + \frac{c_3}{L^2} + \frac{c_4}{L^3} + O\left(\frac{1}{L^4}\right) \ , \tag{4.16}$$

where L represents the size of the system or number of sites, K_2 is the modified Bessel function of the second kind, and c_j and C_j are constant real numbers that depend on the geometry of the system [Far06]. In Fig. 4.6 we use all of the previous energy data points to predict the next ground state energy. As is evident from Fig. 4.6, after some system size our prediction of the energy is well within half of the gap size.

4.5.2.5 Error analysis for numerical calculations

For numerical calculations, the quantity we use to measure the precision of the ground state is the following [Sch11]:

$$\epsilon = \frac{\left|\langle\psi\left|H^2\right|\psi\rangle\right| - \left|\langle\psi\left|H\right|\psi\rangle\right|^2}{\left|\langle\psi\left|H\right|\psi\rangle\right|^2} \, . \tag{4.17}$$

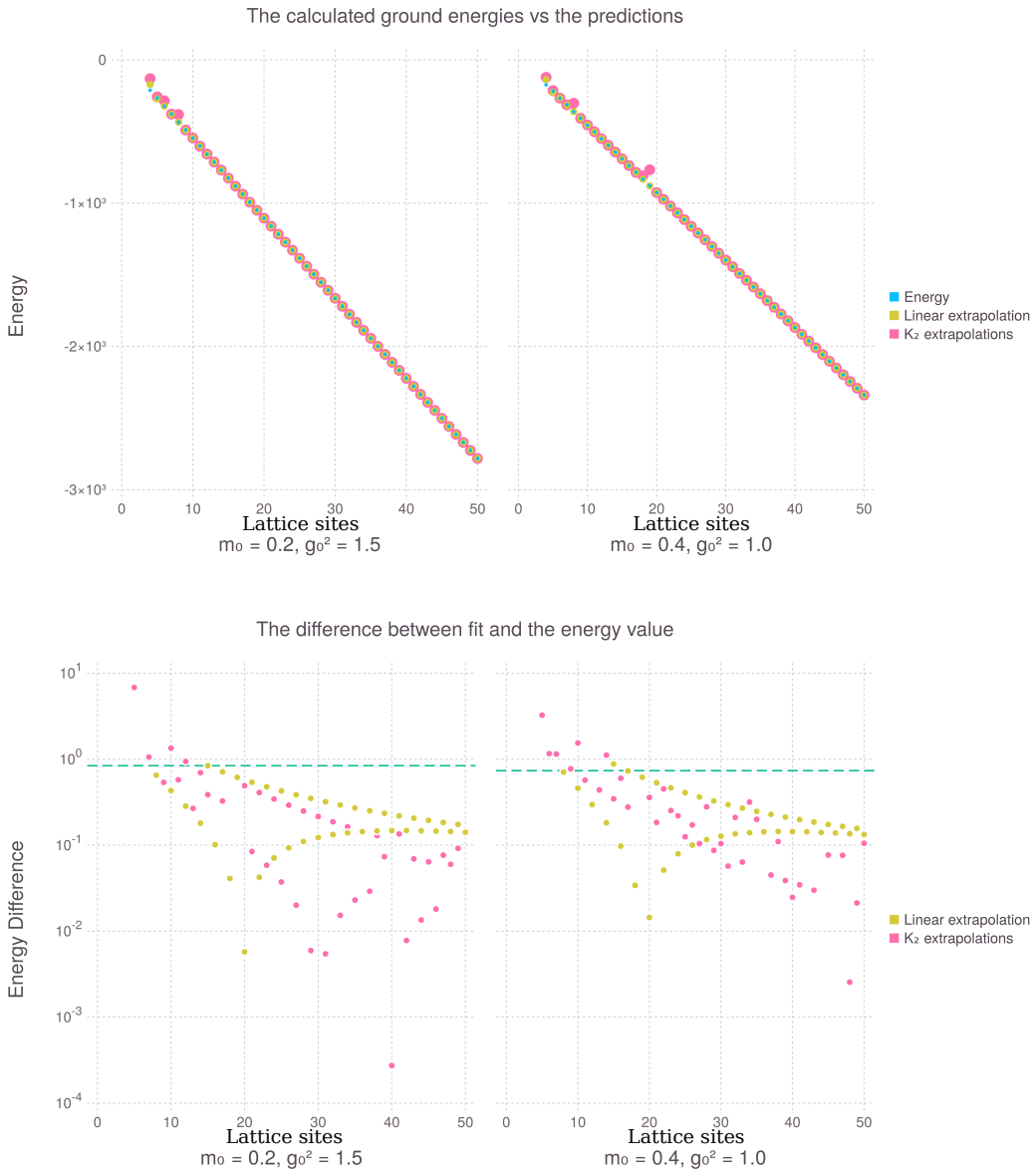

Figure 4.6: (color online) For each data point in this figure, we analyze the energies from previous system sizes by fitting a curve to the values, predicting an energy for the next system size. The top plots show the ground state energies next to the predicted energies, and the bottom plots display the difference between our predictions and the ground state energies. In the asymptotic limit of small systems, the Casimir effect can be approximated by $C_2 \sum_{h=1}^{10} \frac{1}{h^2} K_2 (C_3 h L)$, where L is the system size and C_2 and C_3 are some geometrical constants [Far06]. As one can see, this theoretical argument fits our numerical data too. The mustard dots represent a linear fit, $f(L) = c_0 + c_1 L$ and the pink dots present the difference between the data and $f(L) = C_0 + C_1 L + C_2 \sum_{h=1}^{10} \frac{1}{h^2} K_2 (C_3 h L)$. The dashed teal lines represent the minimum precision required, which is half of the spectral gap, i.e. the renormalized mass. Clearly a linear fit with some estimation for energy density is well within the gap bounds; the higher order fits show the consistency of our calculations.

The DMRG algorithm stops whenever $\epsilon < \epsilon_{\text{goal}}$ or the bond dimension reaches a maximum value, where ϵ_{goal} is the predefined precision goal. We need to know, given a value of ϵ, what the distance between the result of DMRG and the actual ground state is. Let us assume, to the first nonzero order in δ:

$$|\psi\rangle = |g\rangle + \delta|g^{\perp}\rangle \ , \tag{4.18}$$

where $H|g\rangle = E_0|g\rangle$ represents the ground state, $|g^{\perp}\rangle$ is a state orthogonal to the ground state, and δ is a small value. We have:

$$|\langle\psi|H|\psi\rangle| = \left|E_0 + \delta^2 \langle g^{\perp}|H|g^{\perp}\rangle\right| \ \leq \left|E_0 + \delta^2 \langle H\rangle\right| \ , \tag{4.19}$$

$$\left|\langle\psi|H^2|\psi\rangle\right| = \left|E_0^2 + \delta^2 \langle g^{\perp}|H^2|g^{\perp}\rangle\right| \leq \left|E_0^2 + \delta^2 \langle H^2\rangle\right| \ . \tag{4.20}$$

Substituting these values into Eq. (4.17), we get:

$$\begin{aligned} \Rightarrow \epsilon &\approx \delta^2 \left|\frac{\langle H^2\rangle - 2E_0 \langle H\rangle}{E_0^2}\right| \\ &= \delta^2 \left|\left(\frac{E_{\max}}{E_0}\right)^2 - 2\frac{E_{\max}}{E_0}\right| \\ &= \delta^2 \left|\kappa^2 - 2\kappa\right| \ , \end{aligned} \tag{4.21}$$

$$\delta \lessapprox \frac{\sqrt{\epsilon}}{\kappa^2 - 2\kappa} < \sqrt{\epsilon} \ , \tag{4.22}$$

where κ is the condition number of H. δ is upper bounded by $\sqrt{\epsilon}$, and we use this upper bound in our analysis throughout the paper and in Fig. 4.4 for the error bars.

4.6 Conclusion and open problems

In this paper, we have introduced an algorithm that can help with ground state preparation of fermionic QFTs. In particular, our algorithm performs better than state of the art algorithms [HJ18], and it can be generalized to any number of spatial dimensions. Specifically, initialization is no longer the bottleneck of fermionic QFT simulation, as its runtime has the same asymptotic scaling as the rest of the algorithm. Overall, it is a humble step towards answering whether the entirety of the Standard Model can be simulated on a universal digital quantum computer.

It is important to note that although our conjecture about η can be rigorously proven in a number of cases such as systems where the ground state of the theory has a known topological PEPS representation [STV11], whether our algorithm will work for every gapped fermionic system is an open problem.

Also, we believe that the bosonic case needs further investigation and a similar algorithm might work in that case too. One difference one needs to be aware of in that case is that bosonic statistics allow several bosons to occupy the same site and this will necessitate the introduction of a cut-off.

Perhaps a harder open problem to consider is how to generalize these state preparation algorithms to critical systems that lack a mass gap.

Chapter 4: A Glimpse Into the Future

4.1 An Overview Of What We Have Accomplished

> "*You can't connect the dots looking forward; you can only connect them looking backwards. So you have to trust that the dots will somehow connect in your future.*"
>
> Steve Jobs

In this thesis we started by reviewing some of the most influential papers about quantum Hamiltonian simulation algorithms in Chapter 1. We then focused on the specific problem of simulating quantum field theories, specifically the simulation of fermionic quantum field theories. The bottleneck in the known algorithms prior to the results reflected in this thesis, was the state preparation step of the algorithm. That is why we mostly concentrated on that specific part of the algorithm, and in Chapters 3 and 4 introduced new techniques for initial state preparation of fermionic QFTs. By doing so, we improved the expected performance of the fermionic QFT simulation algorithms significantly. In summary we no longer expect state preparation to be the slowest part of the fermionic QFT simulation algorithms.

4.2 Open Problems to Investigate

> "*The significant problems we have cannot be solved at the same level of thinking with which we created them.*"
>
> Albert Einstein

There are plently of problems to be addressed before we can claim that we are ready to simulate a real world complicated quantum field theory simulation problem such as the Standard model. I am going to list the ones that I think can be addressed in near future.

1. Is Conjecture 1 true for all physical fermionic systems? If not what is the criterion that distinguishes between the systems it is true for and the ones it is not. In the meantime it would be helpful to validate it for several other QFTs.

2. How can we apply these recent results from fermionic systems to gauge theories in order to improve the simulation performances. What can we say about hybrid systems that have both fermionic and bosonic fields.

3. In the past few decades there has been a huge effort developing classical numerical tools for strongly interacting theories like Lattice QCD. For example, see [Dav18] and the citation therein. An important question that is worth investigation is that whether the results from these classical calculations can be utilized to do some of the simulation steps more efficiently. E.g. could the spatial two-point correlations be used to prepare the initial states more effi-

ciently? Or could one use some of the LQCD techniques for post-processing the results of the simulation algorithm.

4. Another approach would be to use some of the currently accessible NISQ-era devices to speed up some of the subprocesses in the classical calculations. E.g. can the algorithm for solving linear equations [HHL09] help with some of the internal calculations of LQCD?

5. It might be worth investigating quantum simulation algorithms that live on a dynamic mesh as their underlying discretized lattice. This could allow the simulation algorithm to increase or decrease the lattice whenever it is necessary, and by doing so one might be able to optimize the amount of resources used in the simulation.

6. Chapter 4 predicts the performance of the algorithm to be $O\left(\frac{V^2}{a^{2D}\eta}\,\mathrm{polylog}\,(1/\epsilon)\right)$. As one can observe, the performance is good enough to be a possible candidate for NISQ era calculations. However, in order to be certain one must work out all the constant factors that go into that equation. We will discuss this point further in Sec. 4.3.

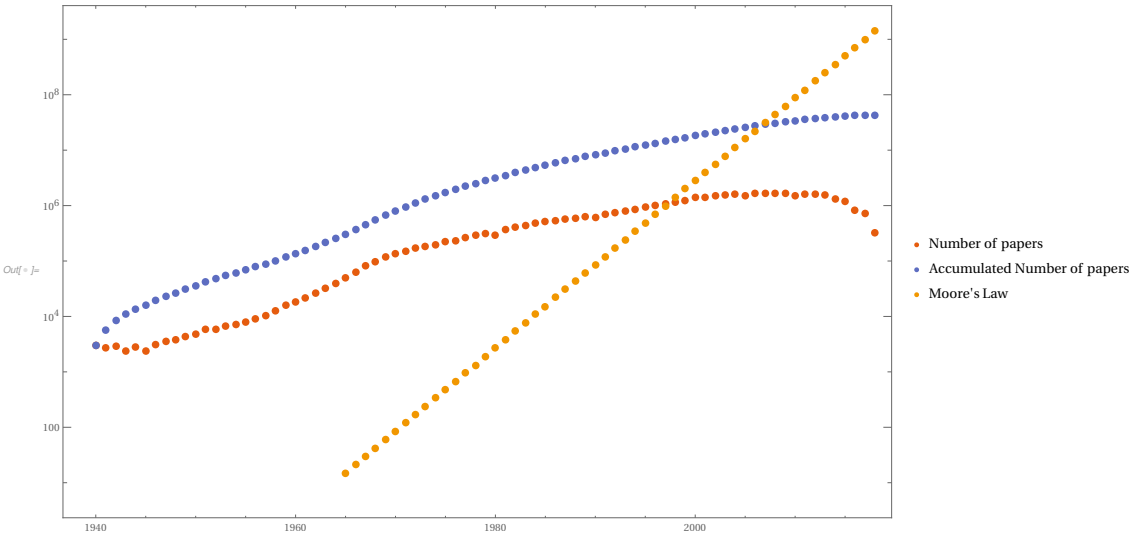

Figure 4.1: (color online) Number of papers that include one of the terms: {"computer","algorithm","programming","coding"} next to Moore's law that predicts the number of transistors in the IC's.

4.3 Predictions

"*There is nothing like a dream to create the future.*"

Victor Hugo

As it is customary, I am going to finish this thesis by making some predictions. Figure 4.1 shows the number of paper related to classical computer's as well as Moore's law for that predicts the number of transistors in integrated circuits (IC), and Fig. 4.2 shows the cumulative number of papers related to quantum computations and quantum algorithms over the years. The number of papers in a field can be thought of as a quantitative figure that represents the amount of knowledge accumulated in a field of study. Figures 4.2 and 4.1 show clear trends of exponential growth.

What is striking is the resemblance between these two plots, the past 30 years

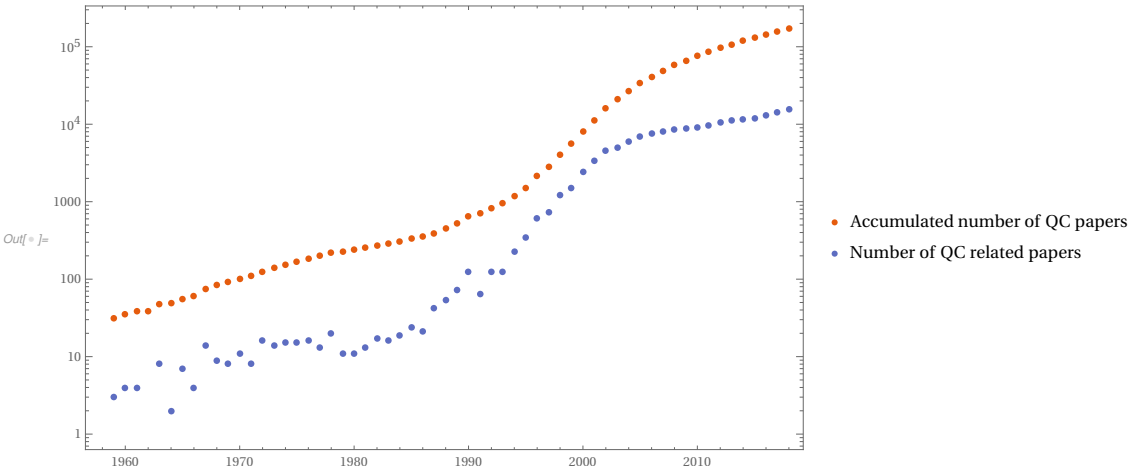

Figure 4.2: (color online) Cumulative number of papers that include at least one of the terms:{"Quantum Computing","Quantum Computer","Quantum Computation","Quantum Algorithm"}. The data was collected via Google Scholar's search engine. The goal of this plot is to roughly represent the amount of knowledge that has been accumulated throughout years in the field of quantum computation. The data suggests that the number of papers is growing by an order of magnitude every 15 years or so.

of quantum computation and 1940's until 1970's for classical computers. One sees that at the beginning of this 30 year period both fields had of the order of 1000 papers and by the end of this 30 year period it has basically grown 2 orders of magnitude. This is good news for researchers that are currently in the field of quantum computation, because if the similarity holds we expect to see continuous growth for the next four or five decades.

Also, the number of qubits that are being reported nowadays (some of the latest results ranging from 53 to 74), is in the same ballpark as the number of transistor on ICs near the end of 1960s. It is easy to predict that the number of addressable qubits will follow the same path as transistors on ICs. If this analogy holds, it is very exciting news, as we should expect a doubling in the number of qubits every two years. This means that within 8 to 10 years we should expect

getting access to 1000 qubits. With 1000 qubits one should be able to simulate a small 3+1 dimensional system that is well beyond the capabilities of any classical computer ever built.

If the analogy holds even further, we can predict that within 20 to 30 years we should expect to see the earliest versions of quantum personal computers. I could push my luck even further and bet on hand-held devices with quantum precessors within 40 years from now, however, because of the intinsic delicacy of quantum systems, I restrain myself from doing so.

Bibliography

[1]B. P. Abbott et al., "Observation of Gravitational Waves from a Binary Black Hole Merger", Physical Review Letters **116**, 061102 (2016).

[2]D. S. Abrams and S. Lloyd, "Simulation of many-body Fermi systems on a universal quantum computer", Physical Review Letters **79**, arXiv:quant-ph/9703054, 2586–2589 (1997).

[3]I. Affleck, T. Kennedy, E. H. Lieb, H. Tasaki, Affleck, Kennedy, Lieb, Tasaki, I. Affleck, T. Kennedy, E. H. Lieb, and H. Tasaki, "Rigorous results on valence-bond ground states in antiferromagnets", Physical Review Letters **59**, 799–802 (1987).

[4]D. Aharonov and A. Ta-Shma, "Adiabatic Quantum State Generation", SIAM Journal on Computing **37**, 47–82 (2007).

[5]D. Aharonov and A. Ta-Shma, "Adiabatic quantum state generation and statistical zero knowledge", in Proceedings of the thirty-fifth acm symposium on theory of computing - stoc '03 (Jan. 2003), p. 20.

[6]M. Aidelsburger, S. Nascimbene, and N. Goldman, "Artificial gauge fields in materials and engineered systems", Comptes Rendus Physique **19**, 394–432 (2018).

[7]I. Arad, Z. Landau, U. Vazirani, and T. Vidick, "Rigorous RG Algorithms and Area Laws for Low Energy Eigenstates in 1D", Communications in Mathematical Physics **356**, 65–105 (2017).

[8]D. Banerjee, M. Bögli, M. Dalmonte, E. Rico, P. Stebler, U. .-.-J. Wiese, and P. Zoller, "Atomic Quantum Simulation of U(N) and SU(N) Non-Abelian Lattice Gauge Theories", Physical Review Letters **110**, 125303 (2012).

[9]J. Banks, J. Carson, B. Nelson, and D. Nicol, *Discrete-event system simulation*, English, 5th ed. (Prentice Hall, 2010).

[10]T. Banks, L. Susskind, and J. Kogut, "Strong-coupling calculations of lattice gauge theories: (1 + 1)-dimensional exercises", Physical Review D **13**, 1043–1053 (1976).

[11]M. C. Bañuls, R. Blatt, J. Catani, A. Celi, J. I. Cirac, M. Dalmonte, L. Fallani, K. Jansen, M. Lewenstein, S. Montangero, C. A. Muschik, B. Reznik, E. Rico, L. Tagliacozzo, K. Van Acoleyen, F. Verstraete, U. .-.-J. Wiese, M. Wingate, J. Zakrzewski, and P. Zoller, "Simulating Lattice Gauge Theories within Quantum Technologies", (2019).

[12]C. D. Batista and G. Ortiz, "Generalized Jordan-Wigner Transformations", Physical Review Letters **86**, 1082–1085 (2000).

[13]H. Bernien, S. Schwartz, A. Keesling, H. Levine, A. Omran, H. Pichler, S. Choi, A. S. Zibrov, M. Endres, M. Greiner, V. Vuletic, and M. D. Lukin, "Probing many-body dynamics on a 51-atom quantum simulator", Nature **551**, 579–584 (2017).

[14]D. W. Berry, G. Ahokas, R. Cleve, and B. C. Sanders, "Efficient quantum algorithms for simulating sparse Hamiltonians", (2005).

[15]D. W. Berry, A. M. Childs, R. Cleve, R. Kothari, and R. D. Somma, "Exponential improvement in precision for simulating sparse Hamiltonians", in Proceedings of the 46th annual acm symposium on theory of computing - stoc '14 (2014), pp. 283–292.

[16]D. W. Berry, A. M. Childs, R. Cleve, R. Kothari, and R. D. Somma, "Simulating Hamiltonian Dynamics with a Truncated Taylor Series", Physical Review Letters **114**, 090502 (2015).

[17]D. W. Berry, A. M. Childs, and R. Kothari, "Hamiltonian Simulation with Nearly Optimal Dependence on all Parameters", in Proceedings - annual ieee symposium on foundations of computer science, focs, Vol. 2015-Decem (Oct. 2015), pp. 792–809.

[18]D. W. Berry, A. M. Childs, Y. Su, X. Wang, and N. Wiebe, "Time-dependent Hamiltonian simulation with L^1-norm scaling", June 2019.

[19]D. W. Berry, R. Cleve, and R. D. Somma, "Exponential improvement in precision for Hamiltonian-evolution simulation", (2013).

[20]D. W. Berry and L. Novo, "Corrected quantum walk for optimal Hamiltonian simulation", (2016).

[21]J. Bezanson, A. Edelman, S. Karpinski, and V. B. Shah, "Julia: A Fresh Approach to Numerical Computing", SIAM Review **59**, 65–98 (2017).

[22]R. Blatt and C. F. Roos, *Quantum simulations with trapped ions*, Apr. 2012.

[23]P. M. Blekher, H. R. Jauslin, and J. L. Lebowitz, "Floquet spectrum for two-level systems in quasiperiodic time-dependent fields", Journal of Statistical Physics **68**, 271–310 (1992).

[24]I. Bloch, J. Dalibard, and S. Nascimbène, *Quantum simulations with ultracold quantum gases*, Apr. 2012.

[25]M. Bordag, U. Mohideen, and V. Mostepanenko, "New developments in the Casimir effect", Physics Reports **353**, 1–205 (2001).

[26]E. T. Campbell, B. M. Terhal, and C. Vuillot, "Roads towards fault-tolerant universal quantum computation", Nature (2017).

[27]E. T. Campbell and D. E. Browne, "On the Structure of Protocols for Magic State Distillation", Lecture Notes in Computer Science 5906 Theory of Quantum Computation, Communication and Cryptography 4th Workshop, TQC 2009, Waterloo, Canada, May 11-13. Page 20 (2009).

[28]E. E. T. Campbell, H. Anwar, and D. E. Browne, "Magic state distillation in all prime dimensions using quantum Reed-Muller codes", Physical Review X, 17–22 (2012).

[29]Y. Cao, A. Papageorgiou, and I. Petras, "Quantum algorithm and circuit design solving the Poisson equation", New Journal of ... (2013).

[30]H. Casini and M. Huerta, "Entanglement entropy in free quantum field theory", Journal of Physics A: Mathematical and Theoretical **42**, 504007 (2009).

[31]J. M. Cerveró and J. D. Lejarreta, "The Floquet analysis and noninteger higher harmonics generation", Journal of Mathematical Physics **40** (1999).

[32]H. Chernoff, "A Measure of Asymptotic Efficiency for Tests of a Hypothesis Based on the sum of Observations", The Annals of Mathematical Statistics **23**, 493–507 (1952).

[33]H. Chernoff, "A Note on an Inequality Involving the Normal Distribution", The Annals of Probability **9**, 533–535 (1981).

[34]A. M. Childs, R. Cleve, E. Deotto, E. Farhi, S. Gutmann, and D. A. Spielman, "Exponential algorithmic speedup by a quantum walk", in Proceedings of the thirty-fifth acm symposium on theory of computing - stoc '03 (Sept. 2003), p. 59.

[35]A. M. Childs and Y. Su, "Nearly optimal lattice simulation by product formulas", Jan. 2019.

[36]A. M. Childs and N. Wiebe, "Hamiltonian simulation using linear combinations of unitary operations", Quantum Information and Computation **12**, 901–924 (2012).

[37]C. B. L. Christof Gattringer, *Quantum chromodynamics on the lattice: an introductory presentation*, 1st ed., Lecture notes in physics 788 (Springer-Verlag Berlin Heidelberg, 2010).

[38]J. I. Cirac and P. Zoller, "Goals and opportunities in quantum simulation", Nature Physics **8**, 264–266 (2012).

[39]L. W. Clark, B. M. Anderson, L. Feng, A. Gaj, K. Levin, and C. Chin, "Observation of Density-Dependent Gauge Fields in a Bose-Einstein Condensate Based on Micromotion Control in a Shaken Two-Dimensional Lattice", Physical Review Letters **121**, 030402 (2018).

[40]S. Coleman, "Quantum sine-Gordon equation as the massive thirring model", Physical Review D **11**, 2088–2097 (1975).

[41]P. C. S. Costa, S. Jordan, and A. Ostrander, "Quantum algorithm for simulating the wave equation", Physical Review A **99**, 012323 (2019).

[42]J. Dalibard, F. Gerbier, G. Juzeliūnas, and P. Öhberg, "Colloquium : Artificial gauge potentials for neutral atoms", Reviews of Modern Physics **83**, 1523–1543 (2011).

[43]M. Dalmonte and S. Montangero, "Lattice gauge theory simulations in the quantum information era", Contemporary Physics **57**, 388–412 (2016).

[44]Z. Davoudi, "Lattice QCD input for nuclear structure and reactions", EPJ Web of Conferences **175**, edited by M. Della Morte, P. Fritzsch, E. Gámiz Sánchez, and C. Pena Ruano, 01022 (2018).

[45]Z. Davoudi, M. Hafezi, C. Monroe, G. Pagano, A. Seif, and A. Shaw, "Towards analog quantum simulations of lattice gauge theories with trapped ions", (2019).

[46]G. De las Cuevas, N. Schuch, D. Perez-Garcia, and J. I. Cirac, "Continuum limits of matrix product states", Physical Review B **98**, 174303 (2018).

[47]C. Deng, F. Shen, S. Ashhab, and A. Lupascu, "Dynamics of a two-level system under strong driving: Quantum-gate optimization based on Floquet theory", Physical Review A **94**, 032323 (2016).

[48]D. Deutsch, "Quantum Computational Networks", Proceedings of the Royal Society A: Mathematical, Physical and Engineering Sciences **425**, 73–90 (1989).

[49]D. Deutsch, "Quantum Theory, the Church-Turing Principle and the Universal Quantum Computer", Proceedings of the Royal Society A: Mathematical, Physical and Engineering Sciences **400**, 97–117 (1985).

[50]D. Deutsch, "Quantum theory, the Church-Turing printicple and the universal quantum computer", Proceedings of the Royal Society of London A **400**, 97–117 (1985).

[51]D. D. P. DiVincenzo and P. W. Shor, "Fault-Tolerant Error Correction with Efficient Quantum Codes", Physical review letters, 1–12 (1996).

[52]C. Farina, "The Casimir effect: some aspects", Brazilian Journal of Physics **36**, 1137–1149 (2006).

[53]R. P. Feynman, "Quantum Mechanical Computers", Optics News **11**, 11 (1985).

[54]R. P. Feynman, "Simulating physics with computers", International Journal of Theoretical Physics **21**, 467–488 (1982).

[55]G. Floquet, "Sur les équations différentielles linéaires à coefficients périodiques", Annales scientifiques de l'École Normale Supérieure **12**, 47–88 (1883).

[56]P. Ginsparg, "Applied Conformal Field Theory", Nov. 1988.

[57]A. W. Glaetzle, M. Dalmonte, R. Nath, I. Rousochatzakis, R. Moessner, and P. Zoller, "Quantum spin-ice and dimer models with Rydberg atoms", Physical Review X **4**, 041037 (2014).

[58]D. González-Cuadra, E. Zohar, and J. I. Cirac, "Quantum simulation of the Abelian-Higgs lattice gauge theory with ultracold atoms", New Journal of Physics **19**, 063038 (2017).

[59]D. Gottesman, "Theory of fault-tolerant quantum computation", Physical Review A **57**, 127–137 (1998).

[60]D. J. Gross and A. Neveu, "Dynamical symmetry breaking in asymptotically free field theories", Physical Review D **10**, 3235–3253 (1974).

[61]J. Haah, M. B. Hastings, R. Kothari, and G. H. Low, "Quantum algorithm for simulating real time evolution of lattice Hamiltonians", arXiv:1801.03922 (2018).

[62]J. Haah, M. B. Hastings, D. Poulin, and D. Wecker, "Magic state distillation with low space overhead and optimal asymptotic input count", Quantum **1**, 31 (2017).

[63]M. Hafezi, A. Sørensen, E. Demler, and M. Lukin, "Fractional quantum Hall effect in optical lattices", Physical Review A **76**, 023613 (2007).

[64]F. D. M. Haldane, "Quantum field ground state of the sine-Gordon model with finite soliton density: exact results", Journal of Physics A: Mathematical and General **15**, 507–525 (1982).

[65]A. Hamed Moosavian, *A DMRG implementation written in Julia*, 2019.

[66]A. Hamed Moosavian and S. Jordan, "Faster quantum algorithm to simulate fermionic quantum field theory", Physical Review A **98**, 012332 (2018).

[67]A. W. Harrow, A. Hassidim, and S. Lloyd, "Quantum Algorithm for Linear Systems of Equations", Physical Review Letters **103**, 150502 (2009).

[68]M. B. Hastings, "An area law for one-dimensional quantum systems", Journal of Statistical Mechanics: Theory and Experiment **2007**, P08024–P08024 (2007).

[69]M. B. Hastings and T. Koma, "Spectral Gap and Exponential Decay of Correlations", Communications in Mathematical Physics **265**, 781–804 (2006).

[70]N. Hatano and M. Suzuki, "Finding Exponential Product Formulas of Higher Orders", Lect. Notes Phys. **679**, 37–68 (2005).

[71]R. Hill, K. W. Masui, and D. Scott, "The Spectrum of the Universe", Applied Spectroscopy **72**, 663–688 (2018).

[72]Y. Huang, "A polynomial-time algorithm for the ground state of one-dimensional gapped Hamiltonians", 1–9 (2014).

[73]D. Jayaweera, *Smart Power Systems and Renewable Energy System Integration*, English, edited by D. Jayaweera, 1st ed. 20, Vol. 57, Studies in Systems, Decision and Control (Springer International Publishing, Cham, 2016).

[74]P. Jordan and E. Wigner, "Über das Paulische Äquivalenzverbot", Zeitschrift für Physik A Hadrons and Nuclei **47**, 631–651 (1928).

[75]S. P. Jordan, H. Krovi, K. S. M. Lee, and J. Preskill, "BQP-completeness of scattering in scalar quantum field theory", Quantum **2**, 44 (2018).

[76]S. P. Jordan, K. S. M. Lee, and J. Preskill, "Quantum Algorithms for Fermionic Quantum Field Theories", Apr. 2014.

[77]S. P. Jordan, K. S. M. Lee, and J. Preskill, "Quantum Algorithms for Quantum Field Theories", Science **336**, 1130–3 (2012).

[78]S. P. Jordan, K. S. M. Lee, and J. Preskill, "Quantum Computation of Scattering in Scalar Quantum Field Theories", Dec. 2011.

[79]D. B. Kaplan, "A method for simulating chiral fermions on the lattice", Physics Letters B **288**, 342–347 (1992).

[80]V. Kasper, F. Hebenstreit, F. Jendrzejewski, M. K. Oberthaler, and J. Berges, "Implementing quantum electrodynamics with ultracold atomic systems", New Journal of Physics **19**, 023030 (2017).

[81]A. Y. Kitaev, "Quantum measurements and the Abelian Stabilizer Problem", arXiv:quant-ph/9511026v1, Nov. 1995.

[82]N. Klco, E. F. Dumitrescu, A. J. McCaskey, T. D. Morris, R. C. Pooser, M. Sanz, E. Solano, P. Lougovski, and M. J. Savage, "Quantum-Classical Computation of Schwinger Model Dynamics using Quantum Computers", Physical Review A **98**, 032331 (2018).

[83]N. Klco and M. J. Savage, "Digitization of scalar fields for quantum computing", Physical Review A **99**, 052335 (2019).

[84]N. Klco and M. J. Savage, "Minimally-Entangled State Preparation of Localized Wavefunctions on Quantum Computers", arXiv:1904.10440 [quant-ph], Apr. 2019.

[85]E. Knill, R. Laflamme, and W. Zurek, "Accuracy threshold for quantum computation", 1–20 (1996).

[86]E. Knill, R. Laflamme, and W. H. Zurek, "Resilient quantum computation: error models and thresholds", Proceedings of the Royal Society of London. Series A: Mathematical, Physical and Engineering Sciences **454**, 365–384 (1998).

[87]J. B. Kogut and L. Susskind, "Hamiltonian formulation of Wilson's lattice gauge theories", Physical Review D **11**, 395–408 (1975).

[88]V. E. Korepin, "Direct calculation of the S matrix in the massive thirring model", Theoretical and Mathematical Physics **41**, 953–967 (1979).

[89]E. H. Lieb and D. W. Robinson, "The finite group velocity of quantum spin systems", Communications in Mathematical Physics **28**, 251–257 (1972).

[90]H.-H. Lin, L. Balents, and M. P. A. Fisher, "Exact SO(8) symmetry in the weakly-interacting two-leg ladder", Physical Review B **58**, 1794–1825 (1998).

[91]S. Lloyd, "Universal Quantum Simulators", Science (New York, N.Y.) **273**, 1073–8 (1996).

[92]G. H. Low and I. L. Chuang, "Hamiltonian Simulation by Uniform Spectral Amplification", arXiv: 1610.06546, 1–32 (2016).

[93]G. H. Low and I. L. Chuang, "Optimal Hamiltonian Simulation by Quantum Signal Processing", Physical Review Letters **118**, 010501 (2016).

[94]G. H. Low, V. Kliuchnikov, and N. Wiebe, "Well-conditioned multiproduct Hamiltonian simulation", (2019).

[95]V. A. Maciej Lewenstein Anna Sanpera, *Ultracold atoms in optical lattices: simulating quantum many-body systems* (Oxford University Press, 2012).

[96]M. Mancini, G. Pagano, G. Cappellini, L. Livi, M. Rider, J. Catani, C. Sias, P. Zoller, M. Inguscio, M. Dalmonte, and L. Fallani, "Observation of chiral edge states with neutral fermions in synthetic Hall ribbons", Science **349**, 1510–1513 (2015).

[97]S. Mandelstam, "Soliton operators for the quantized sine-Gordon equation", Physical Review D **11**, 3026–3030 (1975).

[98]A. M. Meier, B. Eastin, and E. Knill, "Magic-state distillation with the four-qubit code", (2012).

[99]J.-B. Michel, Y. K. Shen, A. P. Aiden, A. Veres, M. K. Gray, J. P. Pickett, D. Hoiberg, D. Clancy, P. Norvig, J. Orwant, S. Pinker, M. A. Nowak, and E. L. Aiden, "Quantitative Analysis of Culture Using Millions of Digitized Books", Science **331**, 176–182 (2011).

[100]A. Micheli, G. Pupillo, H. P. Büchler, and P. Zoller, "Cold polar molecules in two-dimensional traps: Tailoring interactions with external fields for novel quantum phases", Physical Review A **76**, 043604 (2007).

[101]F. Molteni, R. Buizza, T. N. Palmer, and T. Petroliagis, "The ECMWF Ensemble Prediction System: Methodology and validation", Quarterly Journal of the Royal Meteorological Society **122**, 73–119 (1996).

[102]F. Nielsen, "Chernoff information of exponential families", Feb. 2011.

[103]H. B. Nielsen and M. Ninomiya, "A no-go theorem for regularizing chiral fermions", Physics Letters B **105**, 219–223 (1981).

[104]H. Nielsen and M. Ninomiya, "Absence of neutrinos on a lattice", Nuclear Physics B **185**, 20–40 (1981).

[105]M. A. Nielsen and I. L. Chuang, *Quantum Computation and Quantum Information* (Cambridge University Press, 2000).

[106]K. Okunishi, Y. Hieida, and Y. Akutsu, "Universal asymptotic eigenvalue distribution of density matrices and corner transfer matrices in the thermodynamic limit", Physical Review E **59**, R6227–R6230 (1999).

[107]Y. Okwamoto, "Commensurate-Incommensurate Transition in the Two-Dimensional Sine-Gordon System: the Bethe Ansatz Calculation", Journal of the Physical Society of Japan **52**, 942–951 (1983).

[108]L. E. S. (Paul Bratley Bennett L. Fox, *A guide to simulation*, 2nd ed. (Springer-Verlag New York, 1987).

[109]J. R. F. PH.D., *Principles of applied reservoir simulation, third edition*, 3rd ed. (Gulf Professional Publishing, 2005).

[110]J. Preskill, "Reliable quantum computers", Proceedings of the Royal Society of London. Series A: Mathematical, Physical and Engineering Sciences **454**, 385–410 (1998).

[111]J. Preskill, *Simulating quantum field theory with a quantum computer*, Nov. 2018.

[112]M. Pursula, "Simulation of traffic systems : an overview", in (1998).

[113]J. D. Qualls, "Lectures on Conformal Field Theory", Nov. 2015.

[114]B. W. Reichardt, "Improved magic states distillation for quantum universality", QUANT.INF.PROC. **4**, 251 (2005).

[115]B. W. Reichardt, "Quantum universality by state distillation", Quantum Inf Comput **9**, 24 (2006).

[116]E. Rico, M. Dalmonte, P. Zoller, D. Banerjee, M. Bögli, P. Stebler, and U. .-.-J. Wiese, "SO(3) "Nuclear Physics" with ultracold Gases", Annals of Physics **393**, 466–483 (2018).

[117]U. Schollwöck, "The density-matrix renormalization group", Reviews of Modern Physics **77**, 259–315 (2005).

[118]U. Schollwöck, "The density-matrix renormalization group in the age of matrix product states", Annals of Physics **326**, 96–192 (2011).

[119]C. Schön, K. Hammerer, M. M. Wolf, J. I. Cirac, and E. Solano, "Sequential generation of matrix-product states in cavity QED", Physical Review A **75**, 032311 (2007).

[120]C. Schön, E. Solano, F. Verstraete, J. I. Cirac, and M. M. Wolf, "Sequential Generation of Entangled Multiqubit States", Physical Review Letters **95**, 110503 (2005).

[121]N. Schuch, D. Pérez-García, and I. Cirac, "Classifying quantum phases using matrix product states and projected entangled pair states", Physical Review B **84**, 165139 (2011).

[122]M. Schwarz, K. Temme, and F. Verstraete, "Preparing projected entangled pair states on a quantum computer", Physical Review Letters **108**, 110502 (2011).

[123]M. Schwarz, K. Temme, F. Verstraete, D. Perez-Garcia, and T. S. Cubitt, "Preparing topological projected entangled pair states on a quantum computer", Physical Review A - Atomic, Molecular, and Optical Physics **88**, 1–5 (2013).

[124]C. Schweizer, F. Grusdt, M. Berngruber, L. Barbiero, E. Demler, N. Goldman, I. Bloch, and M. Aidelsburger, "Floquet approach to Z2 lattice gauge theories with ultracold atoms in optical lattices", Nature Physics **15**, 1168–1173 (2019).

[125]J. Schwinger, "Gauge Invariance and Mass. II", Physical Review **128**, 2425–2429 (1962).

[126]P. W. Shor, "Fault-tolerant quantum computation", (1996).

[127]P. W. Shor, "Scheme for reducing decoherence in quantum computer memory", Physical Review A **52**, R2493–R2496 (1995).

[128]A. M. Sirunyan et al., "Observation of Higgs Boson Decay to Bottom Quarks", Physical Review Letters **121**, 121801 (2018).

[129]A. M. Steane, "Simple quantum error-correcting codes", Physical Review A **54**, 4741–4751 (1996).

[130]A. Steane, "Multiple Particle Interference and Quantum Error Correction", Proc.Roy.Soc.Lond. A452 (1996) 2551 (1996).

[131]F. Strocchi, "Relativistic Quantum Mechanics and Field Theory", Foundations of Physics **34**, 501–527 (2004).

[132]B. K. Stuhl, H. I. Lu, L. M. Aycock, D. Genkina, and I. B. Spielman, "Visualizing edge states with an atomic Bose gas in the quantum Hall regime", Science **349**, 1514–1518 (2015).

[133]L. Susskind, "Lattice fermions", Physical Review D **16**, 3031–3039 (1977).

[134]M. Suzuki, "General theory of fractal path integrals with applications to many-body theories and statistical physics", Journal of Mathematical Physics **32**, 400–407 (1991).

[135]M. Suzuki, "Generalized Trotter's formula and systematic approximants of exponential operators and inner derivations with applications to many-body problems", Communications in Mathematical Physics **51**, 183–190 (1976).

[136]K. M. Svore, M. B. Hastings, and M. Freedman, *Faster phase estimation*, Apr. 2014.

[137]B. Swingle, "Structure of entanglement in regulated Lorentz invariant field theories", Apr. 2013.

[138]M. Thies and K. Urlichs, "Baryons in massive Gross-Neveu models", Physical Review D **71**, 105008 (2005).

[139]M. Thies and K. Urlichs, "From nondegenerate conducting polymers to dense matter in the massive Gross-Neveu model", Physical Review D **72**, 105008 (2005).

[140]W. G. Unruh, "Maintaining coherence in quantum computers", Physical Review A **51**, 992–997 (1995).

[141]K. Van Acoleyen, M. Mariën, and F. Verstraete, "Entanglement Rates and Area Laws", Physical Review Letters **111**, 170501 (2013).

[142]V. Veitch, S. a. Hamed Mousavian, D. Gottesman, and J. Emerson, "The resource theory of stabilizer quantum computation", New Journal of Physics **16**, 013009 (2014).

[143]G. Vidal, "Efficient Simulation of One-Dimensional Quantum Many-Body Systems", Physical Review Letters **93**, 040502 (2004).

[144]S. R. White, "Density matrix formulation for quantum renormalization groups", Physical Review Letters **69**, 2863–2866 (1992).

[145]K. G. Wilson, "Confinement of quarks", Physical Review D **10**, 2445–2459 (1974).

[146]T. J. Yoder, G. H. Low, and I. L. Chuang, "Fixed-Point Quantum Search with an Optimal Number of Queries", Physical Review Letters **113**, 210501 (2014).

[147]C. Zalka, "Efficient simulation of quantum systems by quantum computers", Proceedings of the Royal Society of London A **454**, arXiv:quant-ph/9603026, 313–322 (1998).

[148]A. B. Zamolodchikov and A. B. Zamolodchikov, "Factorized S-matrices in two dimensions as the exact solutions of certain relativistic quantum field theory models", Annals of Physics **120**, 253–291 (1979).

[149]J. Zhang, G. Pagano, P. W. Hess, A. Kyprianidis, P. Becker, H. Kaplan, A. V. Gorshkov, Z. X. Gong, and C. Monroe, "Observation of a Many-Body Dynamical Phase Transition with a 53-Qubit Quantum Simulator", Nature **551**, 601–604 (2017).

[150]E. Zohar and M. Burrello, "Formulation of lattice gauge theories for quantum simulations", Physical Review D **054506**, 1–15 (2015).

[151]E. Zohar, J. I. Cirac, and B. Reznik, "Quantum simulations of lattice gauge theories using ultracold atoms in optical lattices", Reports on Progress in Physics **79**, 014401 (2015).